DEPARTMENT OF THE INTERIOR

U.S. GEOLOGICAL SURVEY

PETROLOGY, GEOCHEMISTRY AND K-AR AGES OF VOLCANIC-ARC ROCKS DREDGED FROM THE CONTINENTAL MARGIN IN THE BERING SEA

by

Alicé S. Davis, Leda-Beth G. Picktborn, Tracy L. Vallier and Michael S. Marlow

Open-File Report 88-34

This report is preliminary and has not been reviewed for conformity with U.S. Geological Survey editorial standards and stratigraphic nomenclature.

Menlo Park, California

1987

INTRODUCTION

Eocene volcanic rocks with arc characteristics were dredged from the continental margin in the Bering Sea on two U.S. Geological Survey cruises (L5-78-BS and L9-82-BS) in 1978 and 1982. Samples ranging from basalt to rhyolite in composition were recovered from seven sites, and from water depths ranging from 750 to 2200 m. Dredge locations and water depths are listed in Table 1, and dredge locations are shown in Figure 1. Most of the samples appear to be broken-off outcrop, but the rhyolite samples represent isolated, rounded cobbles in a dredge haul composed mostly of sedimentary rock and may be glacial erratics.

This report presents K-Ar ages and petrological and geochemical data for the Eocene volcanic arc rock samples. Strongly alkalic basalt samples of Quaternary age were also recovered in some of the dredges in this area and are described in a separate report (Davis and others, 1987).

METHODS

Samples were studied in thin sections and submitted for bulk chemical analyses to the analytical laboratories of the U.S. Geological Survey. Major element chemistry was determined by wave-length dispersive X-ray fluorescence (XRF) using methods described by Taggart and others (1982). Abundances of Rb, Sr, Zr, Ba, Y, and Nb were determined by energy-dispersive XRF. Precision and accuracy of XRF is 1 to 2% for major elements and 5 to 10% for trace elements. FeO, CO_2, and H_2O were determined by standard wet chemical techniques (Peck, 1964). Abundances of Hf, Ta, Th, Sc, Co, Cr and the rare earth elements (REE) were determined by instrumental neutron activation analysis (INAA) using methods described by Baedecker (1979). Plagioclase, clinopyroxene, orthopyroxene, amphibole and Fe-Ti oxide compositions were determined with a 9-channel electron microprobe, using 15 kv accelerating voltage and 20 nAmp sample current with a narrowly focused beam ($\sim$2 μ) for clinopyroxene, orthopyroxene, amphibole and Fe-Ti oxide, and 15 nAmp and a larger beam size ($\sim$10 μ) for plagioclase. Minerals and synthetic oxides were used as standards. Data reduction was performed using a modified version of the Bence and Albee (1968) program.

For conventional whole-rock K-Ar measurements, rock was crushed and sieved to retain the 0.5 to 1.0 mm size fraction. Plagioclase and amphibole were separated magnetically and with heavy liquids. Plagioclase separates and crushed whole-rock samples were acid-leached with HF and HNO_3 to remove clay alteration products. One aliquant was used for the Ar analysis and another was pulverized to a fine powder for duplicate K_2O analyses. K_2O analyses were performed by flame photometry and Ar mass analyses were done with a multiple collector mass spectrometer. Conventional K-Ar dating techniques used were those described in detail by Dalrymple and Lanphere (1969).

For $^{40}Ar/^{39}Ar$ dating the samples were sealed in air in quartz vials and irradiated in the core of the U.S. Geological Survey TRIGA reactor for 10 to 30 hours where they received a neutron dose of about $1x10^{18}$ to $3x10^{18}$ nvt. Details of $^{40}Ar/^{39}Ar$ techniques are described by Dalrymple and Lanphere (1971) and Dalrymple and others (1981).

PETROGRAPHY AND MINERALOGY

Petrography of the samples is summarized in Table 2 and plagioclase, clinopyroxene, orthopyroxene, amphibole, and Fe-Ti oxide analyses of selected samples are listed in Tables 3, 4, 5, 6 and 7, respectively. The dredged samples comprise basalt, basaltic andesite, andesite, dacite and rhyolite, using the classification scheme of Gill (1981). One of the basaltic samples

(40-8) has the textural features of an intrusive rock with phenocrysts set in a hypidiomorphic-granular groundmass. This sample could be from a gabbroic dike or sill as well as from the interior of a thick flow. However, since textural features reflect mostly mode of emplacement and cooling history this sample is listed as basalt under chemical classification in the tables. One sample (45-7) contains small plagioclase-rich xenoliths, and another (45-4) appears cataclastically sheared with iron oxides filling all fractures. All the samples are at least somewhat altered. Two of the basalt samples (10-2, 10-3) are severely altered, containing metamorphic minerals typical of lower greenschist facies.

Except for the two aphyric meta-basalt samples, all samples are porphyritic. The two rhyolite samples are only sparsely porphyritic with small microphenocrysts of biotite and rare quartz. The biotite is partly replaced by chlorite. Plagioclase is the dominant phenocryst phase in the basalt to dacite suite and may constitute up to 38% of the rock in the more silicic samples. Plagioclase crystals are typically large (to 6 mm) and may be nearly euhedral with slightly rounded corners or they may be anhedral fragments. They typically exhibit strong optical zoning and often contain a "dusty" zone with many tiny inclusions.

Plagioclase compositions in the basalt to dacite suite range from bytownite (An_{82}) to oligoclase (An_{28}), and a compositional range of 30 mol.% in An content is not uncommon in a single thin section (Table 3). The range in Or content in a given sample is considerable, especially in the andesites and dacite (Figure 2). Or increases with decreasing An content in a given sample, and in a general way An correlates with calcium content of the whole rock composition, shifting the range of compositions toward progressively lower An content from basalt to andesite (Figure 2). However, plagioclase compositions in the dacite sample overlap those of the andesites and contain some core compositions as calcic as those in the basalt.

Clinopyroxene occurs in all basalt and andesite samples but is absent in the dacite and rhyolite. Typically, clinopyroxene occurs as anhedral plates or granules, or as very ragged crystal fragments, or more rarely as overgrowth on orthopyroxene. In the andesite samples microphenocrysts of clinopyroxene are rare and very small in size (< 1 mm); in the basalt they are more abundant and larger (to 4 mm). Compositions show a narrow range with a limited iron enrichment trend ($Wo_{37-46}\ En_{44-52}\ Fs_{8-13}$, Table 4, Figure 3). Compositional zoning is minor and commonly normal in basalt with cores more magnesian than rims, whereas zoning in andesite is somewhat larger and may be normal or reverse. TiO_2 is very low, commonly about 0.5%, but ranges from 0.23 to 1.26%. Cr_2O_3 is also typically low, but ranges from 0.05 to 0.87%.

Andesite and dacite samples generally contain some primary orthopyroxene and amphibole. The orthopyroxene (hypersthene) is typically euhedral, colorless to very faintly pinkish-brown pleochroic, with a narrow range in calcium content ($Wo_{1-4}\ En_{67-82}\ Fs_{17-30}$, Table 5, Figure 3). Crystals are either unzoned or have slightly more magnesian cores. Amphibole phenocrysts are either euhedral or broken crystals with some euhedral faces. They are most commonly pleochroic in yellowish or greenish-brown to a deeper brown of the same shade, but some show pale-brown to red-brown pleochroism. Except for one sample (41-6) in which amphibole has largely been replaced by opaque minerals, most amphibole crystals are unaltered, having only thin opaque reaction rims and minor inclusions of iron oxides. Based on the classification of Leake (1978) the amphibole compositions include rare pargasite but range predominantly from edenite or edenitic hornblende to magnesio-hornblende (assuming all iron as FeO). TiO_2 in the amphiboles is typically less than 2% but ranges from 1.24 to 4.0%. Cr and K_2O contents are very low, ranging from 0.0 to 0.09%, and from 0.32 to 1.0%, respectively (Table 6).

Opaque minerals are very abundant in all samples, occurring most commonly as minute specks in the groundmass but also as equant microphenocryst to 1 mm in size. Microphenocrysts, either in the groundmass or included in phenocryst phases, are most commonly

titanomagnetite, but ilmenite is also present (Table 7). The Fe-Ti oxide phases are low in Cr_2O_3 (0.0 to 0.53%), Al_2O_3 (0.05 to 3.6%) and Mg (0.97 to 3.0%), but relatively high in V_2O_3 (0.38 to 1.15%). An ulvospinel component as high as 83% in a titanomagnetite of the dacite sample (40-16) appears too high and may have resulted from the beam overlapping magnetite-ilmenite exsolution lamellae. Other oxide phases in this sample yielded poor analyses with low totals, possibly for the same reason.

Olivine apparently was present in minor amounts in the basalt and some basaltic andesite samples but is completely replaced by iron oxides and clay minerals. A few crystal outlines are clearly indicative of olivine, but some sub- to anhedral pseudomorphs may have been a different mineral phase (pyroxene or amphibole). Other primary minerals include biotite, muscovite and quartz in the rhyolite samples and traces of euhedral apatite in one of the andesite samples. Secondary minerals include chlorite, zeolite, clay minerals, epidote and calcite. Some fractures are filled with sulfide minerals and iron hydroxides.

K-AR AGES

Conventional K-Ar ages were determined for ten plagioclase separates and for two whole-rock samples. Two of the samples, for which conventional K-Ar ages of plagioclase had been determined, were selected for $^{40}Ar/^{39}Ar$ total fusion and incremental heating experiments. The data are presented in Table 8. Preliminary ages for some of these samples have been reported by Marlow and Cooper (1985).

The conventional ages obtained for the plagioclase separates (Table 8a) range from 50.2 ±1.5 to 54.4 ±1.2 Ma. A whole rock age of 49.0 ±1.2 Ma obtained for sample 45-7 is somewhat younger, probably due to alteration, and may be considered a minimum age. A whole rock age of 77 ±1.5 Ma obtained for another sample from the same dredge (45-4) is considerably older than the other samples. This sample apparently is not part of the Eocene arc suite and may be a glacial erratic. Volcanic arc rocks with ages between 66 and 77 Ma have been reported from St. Matthews Island (Patton and others, 1976).

A $^{40}Ar/^{39}Ar$ total fusion age of 56.7 ±3.0 Ma (Table 8b) obtained for the amphibole of sample 40-5 is older than the range of conventional ages obtained for the plagioclase separates. However, it is within 2 standard deviations of the error range for all of the plagioclase analyses, and within 1 standard deviation of the age obtained from the plagioclase of the same sample.

A $^{40}Ar/^{39}Ar$ incremental heating age of 53.0 ±0.5 Ma is concordant with the conventional K-Ar age of 53.3 ±1.3 Ma obtained from the same plagioclase separate. The analytical data for the $^{40}Ar/^{39}Ar$ incremental heating experiment (Table 8b) were interpreted in accordance with the following criteria suggested by Lanphere and Dalrymple (1978):

1) A well-defined, high-temperature age spectrum plateau formed by three or more contiguous gas increments representing at least 50% of the ^{39}Ar released. 2) A well-defined isochron for the plateau points; i.e., a York 2 fit index (SUMS/[N-2]) of less than 2.5. 3) Concordant isochron and plateau ages. 4) An $^{40}Ar/^{36}Ar$ intercept on the isochron diagram not significantly different from the atmospheric value of 295.5 at the 95% level of confidence.

Parameters addressed by these criteria are displayed for various possible combinations of increments in Table 8c. All of these combinations are acceptable with respect to the suggested criteria. We have selected the 710 - 1350 degree set of increments, because it contains the largest number of steps. The age spectrum and isochron plots are displayed in Figure 4. The weighted mean plateau age of 53.0 ±0.5 Ma is concordant with the isochron age of 52.1 ±1.0, and both of these are concordant with the conventional age of 53.3 ±1.3 Ma obtained from the same material. This agreement suggests that these samples are undisturbed, and

that their ages represent the original crystallization ages. The narrow range in ages determined for these samples clearly constrain the time of eruption to the early Eocene.

MAJOR ELEMENT CHEMISTRY

Seventeen samples were analyzed for major and minor elements (Table 9). these samples are classified on basis of dry-reduced SiO_2 contents:

<53 % SiO_2 = basalt
53 - 57 % SiO_2 = basaltic andesite
57 - 63 % SiO_2 = andesite
63 - 70 % SiO_2 = dacite
$>$ 70 % SiO_2 = rhyolite

All samples are at least somewhat altered, with volatile contents ranging from <1.0 to 5.7%. When plotted on a FeO^*/MgO diagram (Figure 5), according to the method of Miyashiro (1974), the samples include tholeiitic and calc-alkalic compositions. All samples with SiO_2 greater than 57% show a distinct calc-alkalic trend. Following the method of Gill (1981), most samples are classified as "medium-K" basalt to dacite, but two samples (15-3, 45-4) are "high-K" basaltic andesite (Figure 6). The two meta-basalt samples and the two rhyolite samples are lower in potassium and are borderline between low-K and medium-K compositions (Table 9, Figure 7). These four samples, in addition to being low in potassium are enriched in sodium, which, in the case of the meta-basalt is most likely the result of spilitization. Low potassium may be a primary feature of the rhyolites reflecting biotite fractionation or may have resulted from secondary alteration. The rhyolite compositions fall along the calc-alkalic trend defined by the basaltic andesite to dacite suite (Figures 5,6,7). TiO_2, CaO, and Al_2O_3 generally decrease with increasing SiO_2, whereas Na_2O increases (Figure 7), but all oxides show considerable scatter, especially in the basaltic range. Relatively high Al_2O_3 and low TiO_2 abundances are commonly observed in island arc compositions. The calc-alkalic compositions have typical island arc characteristics, but some of the tholeiitic samples (10-2,10-3, 45-4, 47-8) have higher TiO_2 and lower Al_2O_3 contents, resembling ocean floor basalt, although TiO_2 content is still well within the range observed for arc compositions.

TRACE ELEMENT CHEMISTRY

Abundances of twenty trace elements for the seventeen samples are presented in Table 10. Except for the spilitized basalt samples, Rb, Sr, and Ba abundances are high and extremely variable, ranging from 13 to 50, 325 to 843, and 230 to 1360 ppm, respectively. The spilitized basalt samples have very low Rb (2 ppm) and low Sr (120, 132 ppm) abundances similar to ocean ridge basalt. Ba abundances (80 and 104) are also much lower than in any of the other samples, but somewhat higher than typical ocean ridge basalt. However, these elements are easily mobilized by secondary alteration processes. High-field-strength elements like Zr, Nb, Hf, and Ta that are more resistant to alteration (e.g. Winchester and Floyd, 1976; Wood and others, 1976) are generally lower than in equivalently differentiated ocean ridge basalt. Depletion in Nb and Ta is characteristic of island arc lavas. On a Th-Hf-Ta plot (Figure 8) all samples except the spilitized basalt (10-2, 10-3) plot in the field for convergent plate margins.

Rare earth elements (REE) also show a considerable range in compositions with La/Yb ratios ranging from 2.0 to 14.0 in the basalt to dacite suite, and as high as 17 to 20 in the rhyolites. The chondrite-normalized REE compositions fall into two distinct groups: One

relatively flat for the basalt samples (Fig. 9a), the other, consisting of more silicic samples (>53% SiO_2), has steeper slopes with enriched light REE (LREE) and lower heavy REE (HREE) abundances (Figure 9b). The generally flat patterns of the spilitized basalt samples (Figure 9c) show several erratic spikes in the lighter REE region, indicative of secondary alteration. The rhyolite samples have very steep profiles with extremely low HREE abundances (Figure 9d).

The presence of relatively flat patterns for tholeiitic basalt and one with steeper slopes for the calc-alkalic suite has been observed in other island arc samples (e.g. Basaltic Volcanism Project, 1981; Kay and others, 1982; Whitford and others, 1979). None of the basalt samples show the severe light REE depletion of the "classical" island arc tholeiite of Jakes and Gill (1970) and Jakes and White (1972). However, the pronounced enrichment of Ba over light REE is a distinctive feature of all island-arc lavas. A plot of chondrite-normalized $(Ba/La)_N$ vs. $(La/Sm)_N$ shows all of the samples, except 10-2, well above the field for oceanic basalt (Figure 10). Sample 40-8, which may be a gabbroic dike rock, has such a high $(Ba/La)_N$ ratio ($\sim$27) that it falls outside Figure 10. The abnormally high Ba contents of this sample may have resulted from contamination by wallrock.

COMPARISON WITH OTHER ISLAND ARC COMPOSITIONS

Except for the meta-basalt, the samples dredged from the Beringian margin clearly have volcanic arc affinities. The two meta-basalt samples may represent ocean floor on which the volcanic arc was built; however an origin as arc tholeiite cannot entirely be ruled out. Low Ti, Nb, Ta and high Ba abundances relative to LREE are similar to compositions from volcanic arcs in general (e.g. Basaltic Volcanism Project, 1981; Gill, 1981). Likewise, abundance of strongly zoned plagioclase, presence of two pyroxenes and primary amphibole are mineralogical features shared with many volcanic arc andesites. Chemically, all three volcanic suites commonly occurring in close association in many volcanic arcs, that is tholeiitic, calc-alkalic and shoshonitic, appear to be represented.

The dredged samples show a strong similarity to modern Aleutian arc compositions. Two broad magmatic trends, tholeiitic and calc-alkalic, are recognized for Aleutian volcanoes (Kay and others, 1982). Tholeiitic and calc-alkalic differentiation trends are distinguished on basis of FeO^*/MgO vs. SiO_2 (Figure 5) in which the tholeiitic trend shows iron enrichment with increased differentiation, whereas the calc-alkalic trend shows very little change in FeO^*/MgO over a large range in SiO_2. With more silicic compositions (>54% SiO_2) the distinction between these two trends becomes very apparent (Figure 5); however in the range of basaltic compositions these fields overlap. Individual volcanic centers may erupt lavas with characteristics of both trends. Furthermore, early Tertiary lava from the Aleutians shows the same compositional diversity (Rubenstone, 1984), indicating that this magmatic diversity has persisted since inception of the arc. The dredged andesite and dacite correspond to the calc-alkalic trend of Aleutian volcanoes. Major element trends of dredged samples are similar to those from the Aleutians (Figure 6,7), however, the high-K basaltic andesite sample (15-3) lies outside the field for modern Aleutian arc compositions, but resembles the shoshonitic trend observed in subduction-related volcanic suites in Alaska (Moll-Stalcup, 1987) and in many other volcanic arcs (Gill, 1981). No shoshonitic lavas have erupted along the major volcanic axis in the Aleutians (Kay and others, 1982), but the island of Bogoslof, located a short distance behind the arc, has erupted high-K basalts and andesites (Arculus and others, 1976). Compositons of three lava flows from Bogoslof Island are shown for comparison on Figures 5,6, and 7, and show similar K_2O content as the high-K sample dredged from the Beringian margin. However, TiO_2 content of Bogoslof samples appears somewhat lower at a comparable SiO_2 range.

REE abundances of Aleutian lavas show similar chondrite-normalized patterns as the dredged samples, namely profiles that are relatively flat in the basaltic range, especially for tholeiitic samples, and profiles that become steeper, showing LREE over HREE enrichment in the calc-alkalic andesite to dacite range. However, the calc-alkalic andesite and dacite compositions of the dredged samples have steeper slopes and lower heavy REE abundances than Aleutian lavas of comparable SiO_2 content, suggesting that garnet and amphibole may have played a larger role in the petrogenesis of these samples. The dredged samples show no significant Eu anomaly, whereas some Aleutian samples with >59% SiO_2 show distinctive negative or positive Eu anomalies (Kay and others, 1982). Mineral compositons of plagioclase, clino- and orthopyroxene and amphibole in dredged samples overlap with those reported for Aleutian lavas, except that some amphibole crystals in the dredged samples show some higher values in TiO_2 and lower Al_2O_3 (Kay and Kay, 1985; Rubenstone, 1984).

Volcanic rocks with features characteristic of subduction-related arc rocks, similar to the samples dredged from the Beringian margin, are abundant throughout Alaska. A broad belt of arc-type magmatism, consisting predominantly of medium-K and high-K basalt to rhyolite, spans a distance of more than 550 km in western Alaska (Moll-Stalcup, 1987). Conventional whole-rock K-Ar ages determined for samples within this belt range from 75 to 56 Ma (Moll-Stalcup, 1987). Unlike the modern Aleutian arc lavas, shoshonitic compositions are abundant in the northern part of this belt and may reflect a continental influence, as does the presence of rhyolite, which appears to be rare in intra-oceanic arcs. Comprehensive data sets, including well-constrained K-Ar data, major, trace and mineral chemistry for these Alaskan rocks are exceedingly rare, and hence a detailed comparison between these rocks and the dredged rocks is not possible.

CONCLUSIONS

Samples dredged from several locations along the Beringian margin are clearly of volcanic arc origin, implying a convergent history for this region during the early Tertiary. Compositionally the dredged samples show no significant differences from those presently erupted in the Aleutian arc. They also resemble many of the rocks from western Alaska that have arc-compositions, although chemical diversity and a much greater range in ages are observed for the Alaskan rocks. Well constrained K-Ar ages limits the age of the dredged samples between 55 and 50 Ma, which is considerable younger than arc type volcanism on St. Matthews Island (65 to 77 Ma; Patton and others, 1976). Hence, these samples do not appear to be part of that belt, but instead appear to be part of a younger belt of arc-type magmatism farther south. The oldest lavas erupted from the Aleutian arc appear to approach 50 Ma in age (Rubenstone, 1984), suggesting that the site of convergence shifted to its present position at about 50 Ma.

Recent volcanism along the Beringian margin ranges from about 2 m.yrs. to < 100,000 yrs. (Cox and others, 1966; Lee-Wong and others, 1979; Davis and others, 1987), and shows no similarity with island arc volcanism, but rather consists of strongly alkalic (not shoshonitic) basalt similar to that erupted during the rejuvenated stage of volcanism on oceanic islands or in continental settings. In either setting, this type of volcanism appears to be related to tectonic activity involving normal faulting and uplift or subsidence (Davis et al., 1987).

Eocene arc volcanic rocks from the Beringian margin may be either part of an allochthonous terrane accreted to the continental margin, or they may be an autochthonous volcanic arc, which was the site of convergence during the early Eocene. There appears to be no evidence for large transform faults in this region. Subduction-related rocks occurring along the continental margin extend over a total distance of more than 600 km, if the Eocene arc-related intrusives on St. George Island are included (Barth, 1956; Vallier unpulished data). In

addition seismic data suggests a thick sediment wedge (9-10 km) appears to be buried beneath the continental margin (Marlow and Cooper, 1985) which may be a trench deposit. Therefore, we prefer to interpret the data as representing the youngest arc in a series of belts of arc-type magmatism in this region. Plate motion studies of the North Pacific (Scholl and others, 1986) and age data from the Aleutian arc (Rubenstone, 1984) suggest that the site of convergence shifted to the Aleutian arc in the 55 to 50 Ma interval. Thus these rocks appear to represent the last pulse in arc-type magmatism during the last stages of convergence before relocating subduction to its present position at the Aleutian arc.

REFERENCES

Arculus, R.J., Delong, S.E., Kay, R.W., Brooks, C. and Sun, S.S., 1976, The alkalic rock suite of Bogoslof Island, eastern Aleutian Arc, Alaska. J. Geology, v.85, p.177-186.

Baedecker, P.A., 1979, The INAA program of the U.S. Geological Survey (Reston, Virginia), in Carpenter and others, eds., Computers in activation analysis and γ-ray spectroscopy: Conf.-78042, U.S. Department of Energy, p. 373-385

Barth, T.F.W., 1956, Geology and petrology of the Pribilof Islands, Alaska, in Investigations of Alaskan volcanoes: U.S. Geol. Bull. 1028F, p. 101-160.

Basaltic Volcanism Project, 1981, Basaltic volcanism on the terrestrial planets. Pergamon Press, New York, 1286 pp.

Bence, A.E. and Albee, A.E., 1968, Empirical correction factors for the electron microanalysis of silicates and oxides: J. of Geol., v. 76, p. 382-403.

Cox, A., Hopkins, D.M., and Dalrymple, G.B., 1966, Geomagnetic polarity epochs: Pribilof Islands, Alaska: Geol. Soc. Am. Bull., v.77, p. 883-910.

Dalrymple, G.B. and Lanphere, M.A., 1969, Potassium-Argon Dating: San Francisco, W.H. Freeman Co., 258 p.

Dalrymple, G.B. and Lanphere, M.A., 1971, $^{40}Ar/^{39}Ar$ technique of K-Ar dating: A comparison with the conventional technique. Earth and Planet. Sci. Lett., v.12, p.300-308.

Dalrymple, G.B., Alexander, E.C., Lanphere, M.A. and Kraker, G.P., 1981, Irradiation of samples for $^{40}Ar/^{39}Ar$ dating using the Geological Survey TRIGA reactor. U.S. Geol. Survey Prof. Paper 1176, pp.55.

Davis, A.S., Wong, F.L., Pickthorn, L.B.G., and Marlow, M.S., 1987, Petrology, geochemistry and age of basanitoids dredged from the Bering Sea continental margin west of Navarin Basin. U.S. Geological Survey Open-File Report 87-407, 31 pp.

Gill, J., 1981, Orogenic andesites and plate tectonics. Springer Verlag, N.Y., 390 pp.

Jakes, P. and Gill, J., 1970, Rare earth elements and the island arc tholeiitic series. Earth Planet. Sci. Lett., v.9, p.17-28.

Jakes, P. and White, A.J.R., 1972, Major and trace element abundances in volcanic rocks from orogenic areas. Bull. Geol. Soc. Am., v.83, p.29-40.

Kay, S.M., Kay, R.W. and Citron, G.P., 1982, Tectonic controls on tholeiitic and calc-alkaline magmatism in the Aleutian arc. J. Geophys. Res., v.87, p.4051-4072.

Kay, S.M. and Kay, R.W., 1985, Aleutian tholeiitic and calc-alkaline magma series I: The mafic phenocrysts. Contrib. Mineral. Petrol., v.90, p.276-290.

Lanphere, M.A. and Dalrymple, G.B., 1978, The use of $^{40}Ar/^{39}Ar$ data in evaluation of disturbed K-Ar systems. in Zartman, R.E. (Ed.), Short papers of the fourth International Conference, Geochronology, Cosmochronology, Isotope Geology. U.S. Geol. Survey

Open-File Report 78-701, p.241-243.

Leake, B.E., 1978, Nomenclature of amphiboles. Mineral. Mag., v.63, p.1023-1052.

Lee-Wong, F., Vallier, T.L., Hopkins, D.M. and Silberman, M.L., 1979, Preliminary report on the petrography and geochemistry of basalts from the Pribilof Islands and vicinity, southern Bering Sea: U.S. Geol. Survey Open-File Report 79-1556, 51p.

Marlow, M.S. and Cooper, A.K., 1985, Regional geology of the Beringian margin. in Nasu, N. and others (Eds.) Formation of active ocean margins. Terra Scien. Pub. Co., Tokyo, p.497-515.

Masuda, A. and Nakamura, N., 1973, Fine structures of mutually normalized rare-earth patterns of chondrites. Geochim. Cosmochim. Acta, v.37, p.239-248.

Miyashiro, A., 1974, Volcanic rock series in island arcs and active continental margins. Am. J. Sci., v.274, p.321-355.

Moll-Stalcup, E., 1987, Cenozoic magmatism in mainland Alaska: in Alaskan Geology: DNAG, Geol. Soc. Am. (in press).

Patton, W.W., Lanphere, M.A., Miller, T.P. and Scott R.A., 1976, Age and significance of volcanic rocks on St. Matthew Island, Bering Sea, Alaska. U.S. Geological Survey Jour. Res., v.4, p.67-73.

Peck, L.C., 1964, Systematic analysis of silicates: U.S. Geol. Survey Bull. 1170, 84p.

Rubenstone, J.L., 1984, Geology and geochemistry of early Tertiary submarine volcanic rocks of the Aleutian Islands, and their bearing on the development of the Aleutian island arc. Ph.D. thesis, Cornell University, Ithaca, N.Y. 352 pp.

Scholl, D.W., Vallier, T.L., and Stevenson, A.J., 1986, Terrane accretion, production and continental growth: a perspective based on the origin and tectonic fate of the Aleutian-Bering Sea region. Geology, v.14, p.43-47.

Taggart, J.E., Lichte, F.E. and Wahlberg, J.S., 1982, Methods of analysis of samples using x-ray fluorescence and induction-coupled plasma spectroscopy, in The 1980 Eruptions of Mount St. Helens, Washington: U.S. Geol. Survey Prof. Pap. 1250, p. 683-687.

Winchester, J.A. and Floyd, P.A., 1976, Geochemical magma type discrimination: application to altered and metamorphosed basic igneous rocks. Earth Planet. Sci. Lett., v.28, p.449-469.

Whitford, D.J., Nicholls, I.A. and Taylor, S.R., 1979, Spatial variations in the geochemistry of Quaternary lavas across the Sunda arc in Java and Bali. Contrib. Mineral. Petrol., v.70, p.341-356.

Wood, D.A., Gibson, I.L. and Thompson, R.N., 1976, Elemental mobility during zeolite facies metamorphism of the Tertiary basalts of eastern Iceland. Contrib. Mineral. Petrol., v.55, p.241-254.

Wood, D.A., 1980, The application of a Th-Hf-Ta diagram to problems of tectonomagmatic classification and to establishing the nature of crustal contamination of basaltic lavas of

the British Tertiary volcanic province: Earth Planet. Sci. Lett., v.50, p. 11-30.

Table 1: Dredge Locations

Cruise I.D.	Dredge No.	Location (Lat. ° N)	Location (Long. ° W)	Water depth (m)
L5-78-BS	10	58 ° 20.2'	174 ° 51.7'	1450-1800
L5-78-BS	15	58 ° 27.5'	176 ° 51.9'	950-1100
L5-78-BS	22	59 ° 36.9'	178 ° 49.2'	1500-2200
L9-82-BS	40	58 ° 36.1'	177 ° 20.9'	800-1950
L9-82-BS	41	58 ° 36.6'	177 ° 20.7'	750
L9-82-BS	45	58 ° 31.7'	176 ° 11.4'	840-1400
L9-82-BS	47	58 ° 31.6'	176 ° 04.9'	900-1400

Table 2: Summary of Petrographic Data

Sample No.	Rock Type	Texture	Phenocrysts vol.%*	Minerals	vol.%*	Groundmass Minerals	Remarks
10-2	Meta-basalt low-K tholeiitic	intergranular to intersertal	0	aphyric	100	plag > chlor > epi > opq	metamorphosed to greenschist facies
10-3	Meta-basalt low-K tholeiitic	intergranular to intersertal	0	aphyric	100	plag > epi > chlor > opq	metamorphosed to to greenschist facies
15-3	B.Andesite High-K tholeiitic	pilotaxitic	17 4 Tr	plag cpx oliv	79	plag > opq > cpx > clay + Fe hydroxides	olivine pseudomorphed by sapouite
15-5	Basalt med-K calc-alk.	seriate	8 2 Tr	plag. cpx oliv	85	plag > cpx > opq > clay + Fe hydroxides	subhedral plagioclase anhedral cpx to ~2mm to ~2 mm
15-6	Basalt med-K calc-alk.	seriate	5 3 Tr	cpx plag oliv?	90	plag > cpx > clay + Fe hydroxide> opq	~2% vesicles plagioclase altered, anhedral cpx to 8mm
15-7	Basalt low-K tholeiitic	intergranular to intersertal	18 7 Tr	plag cpx oliv?	70	plag > cpx > clay + Fe hydrox.> opq	~5% vesicles + vugs plagioclase euhedral with minor inclusions
22-10	Rhyolite low-K calc-alk.	v. fine-grnd. holocrystalline	4 1	biotite quartz	94	microcrystalline intergrowth of qtz and feldspar	biotite largely replaced by chlorite
22-11	Rhyolite low-K calc-alk.	v. fine-grnd. holocrystalline	1 Tr	biotite quartz	99	microcrystalline qtz + feldspar bio. + opq	biotite largely replaced by chlorite
40-5	Andesite med.-K calc-alk.	hyalopilitic to intersertal	38 10 5	plag amph opx	46	cryptocrystalline to perlitic glass opq abundant	plagioclase euhedral to subhedral to 4mm cpx anhed., opx euh.
40-6	Andesite med.-K calc.-alk.	pilotaxitic to intersertal	37 8 2 Tr	plag amph opx cpx	53	plag > amph > cpx > clays	rare vugs, plagioclase dusky, cpx overgrowth on opx, amphibole yellow to red-brown

Table 2: Summary of Petrographic Data (continued)

Sample No.	Rock Type	Texture	Phenocrysts vol.%	Minerals	Groundmass vol.%	Minerals	Remarks
40-7	Andesite — calc-alk.	pilotaxitic	30 8 2	plag amph opx	59	plag > amph > opq > cpx	plagioclase to 4 mm amphibole rimmed by opaques
40-8	Basalt (Gabbro) med.-K calc-alk.	allotriomorphic granular	12 5 2	cpx oliv? plag	80	plag > cpx > opq ~ clay + chlorite	plagioclase to 2mm, cpx anhedral to 4mm sector-zoned
40-9	Andesite med-K calc-alk.	pilotaxitic to intersertal	28 8 3 1	plag amph opx opq	60	cryptocrystalline groundmass > amph > opq > cpx	abundant broken plagio- clase, amphibole yellow to green-brown pleochroic
40-10	Andesite med-K calc-alk.	pilotaxitic	32 10 2 <1	plag amph opx Cpx	55	microcrystalline groundmass with plag. microlites opq + broken amph	rare vugs with zeolites, amphibole with opaque rims
40-16	Dacite med-K calc-alk.	intersertal	24 8 3	plag amph opx	75	plag. in brown cryptocrystalline groundmass	plagioclase clean to 6 mm amphibole khaki-green to brown pleochroic
41-6	Andesite med-K calc-alk.	trachytic	15 5 2	plag amph? opq	77	plag > opq > cpx trace of apatite and orthoclase	plagioclase mod. altered, amphibole mostly re- placed by opaques
45-4	B.Andesite High-K tholeiitic	intergranular	12	plag	88	plag > opq > cpx	cataclastic, all fractures filled with opaques
45-7	Andesite med-K calc-alk.	subtrachytic to intergranular	<1	plag	99	plag > cpx > opq	small plag.-rich xeno- liths present with minor cpx + opaques.
47-8	Basalt med-K tholeiitic	subtrachytic to intergranular	15 2 Tr	plag oliv? opq	83	plag > cpx > opq abndt. brown clays	highly altered ~8% irreg.-shaped vugs

* volume percent visually estimated, plag= plagioclase, cpx= clinopyroxene, opx= orthopyroxene, opq= opaque minerals, oliv= olivine, epi= epidote, chlor= chlorite, amph= amphibole

Table 3: Plagioclase Analyses

Sample No.	15-5 1R	15-5 1C	15-5 2mc	15-5 3C	15-5 3R	15-5 4R	15-5 4C	15-5 5mc	40-5 1R	40-5 1C	40-5 2mc	40-5 3mc	40-5 4R	40-5 4C	40-6 1R	40-6 1I	40-6 1C	40-6 2R	40-6 2C	40-6 3mc	40-6 4mc	40-6 1mc
wt.%																						
SiO_2	53.0	53.1	54.7	52.3	52.6	52.3	53.5	51.2	60.8	60.8	58.1	52.7	59.0	60.2	59.7	58.1	58.4	60.0	59.4	52.3	55.0	52.2
Al_2O_3	28.7	29.2	27.8	29.1	28.0	28.9	28.3	29.7	24.6	23.7	25.5	28.9	24.8	24.4	24.6	27.2	25.9	24.5	25.1	29.3	26.5	29.0
FeO	0.33	0.35	0.74	0.71	0.75	0.80	0.77	0.80	0.25	0.25	0.28	0.84	0.26	0.29	0.27	0.28	0.22	0.25	0.27	0.84	0.71	0.68
MgO	0.18	0.17	0.10	0.15	0.17	0.13	0.14	0.28	0.01	0.01	0.02	0.11	0.01	0.02	0.00	0.01	0.02	0.02	0.02	0.13	0.21	0.10
CaO	12.4	12.5	10.8	13.5	13.5	12.7	12.0	13.6	6.48	5.82	8.10	13.6	7.59	6.94	6.88	9.58	7.59	6.63	6.83	12.7	9.84	13.5
Na_2O	4.30	4.35	5.29	4.12	4.25	4.00	4.44	3.63	7.51	7.84	6.83	4.30	7.13	7.31	7.35	5.09	7.06	7.59	7.36	4.24	5.54	4.23
K_2O	0.31	0.29	0.39	0.33	0.32	0.33	0.41	0.21	0.44	0.45	0.31	0.14	0.37	0.40	0.36	0.22	0.36	0.37	0.37	0.19	0.41	0.25
Total	99.5	100.3	99.7	99.3	99.5	99.2	99.5	99.5	99.5	98.9	99.2	99.4	99.2	99.4	99.0	99.3	99.5	99.3	99.3	99.4	98.3	99.0
mol.%																						
An	60.3	60.3	51.4	61.6	60.7	62.5	58.5	66.6	31.5	28.3	38.9	61.3	36.3	33.6	32.7	46.3	36.7	31.9	33.1	61.5	48.3	49.0
Ab	37.9	38.0	46.3	36.5	37.4	35.5	39.1	32.2	66.0	69.1	59.3	37.9	61.7	64.1	65.2	52.4	61.6	66.0	64.8	37.3	49.2	49.0
Or	1.8	1.7	2.2	1.9	1.9	2.0	2.4	1.2	2.6	2.6	1.8	0.8	2.1	2.3	2.1	1.3	1.7	2.1	2.1	1.1	2.4	1.9

Sample No.	40-8 2R	40-8 2C	40-8 3R	40-8 3C	40-8 4mc	40-10 1R	40-10 1I	40-10 1C	40-10 2mc	40-10 3R	40-10 3C	40-10 4R	40-10 4C	40-10 5mc	40-10 6R	40-10 6C	40-16 1R	40-16 1C	40-16 2mc	40-16 3R	40-16 3C	40-16 4mc	40-16 5mc
wt.%																							
SiO_2	51.7	50.0	53.7	47.7	55.1	59.9	59.6	60.1	53.8	55.9	56.4	60.7	58.5	58.1	60.4	61.0	58.5	57.2	56.7	59.5	59.8	57.5	57.5
Al_2O_3	30.2	31.8	27.9	32.1	27.7	24.8	24.9	24.7	28.8	27.1	27.5	24.2	25.8	27.7	24.8	24.3	25.3	26.5	25.9	24.8	24.7	26.1	26.3
FeO	0.77	0.75	0.68	0.74	0.84	0.22	0.22	0.24	0.53	0.48	0.44	0.27	0.20	0.23	0.27	0.21	0.28	0.27	0.27	0.26	0.26	0.33	0.33
MgO	0.10	0.10	0.11	0.12	0.08	0.01	0.02	0.02	0.06	0.07	0.06	0.02	0.02	0.04	0.02	0.03	0.02	0.03	0.03	0.02	0.03	0.03	0.03
CaO	13.4	14.5	11.7	16.8	10.4	6.91	6.99	6.84	11.5	9.92	9.94	6.55	7.50	9.88	6.81	6.29	7.61	8.65	8.98	6.96	7.02	8.56	8.54
Na_2O	3.79	3.24	4.87	1.99	5.33	7.35	7.40	7.38	4.98	5.77	5.78	7.84	7.14	5.84	7.48	7.67	7.61	6.65	6.22	7.32	7.14	5.46	5.50
K_2O	0.20	0.15	0.31	0.08	0.36	0.40	0.40	0.42	0.17	0.23	0.24	0.39	0.29	0.21	0.37	0.41	0.35	0.25	0.25	0.39	0.38	0.24	0.22
Total	100.0	99.8	99.1	99.3	99.7	99.8	99.8	99.6	99.3	99.5	100.3	99.7	99.8	100.0	100.1	99.9	99.0	99.2	98.5	99.2	99.3	99.1	99.4
mol.%																							
An	65.3	70.7	57.1	81.7	50.9	33.4	33.5	33.1	55.5	48.1	48.1	31.4	36.1	47.7	32.1	30.4	36.9	42.0	43.7	33.6	34.4	41.7	41.5
Ab	33.8	28.5	41.2	17.8	47.1	64.3	64.2	64.6	43.5	50.6	50.5	66.4	62.2	51.0	65.7	67.2	61.0	56.5	54.9	64.1	63.3	56.9	57.2
Or	1.2	0.9	1.8	0.5	2.1	2.3	2.3	2.4	1.0	1.3	1.4	2.2	1.7	1.2	2.1	2.4	2.0	1.5	2.3	2.4	1.0	1.3	1.4

mc= core of small crystal

R= rim of larger crystal

C= core of larger crystal

I= intermediate position between rim and core

Table 4: Clinopyroxene Analyses

Sample	15-5 1R	15-5 1C	15-5 2R	15-5 2C	15-5 3mc	40-5 1R	40-5 1C	40-5 2mc	40-5 3mc	40-6 1mc	40-6 2R	40-6 2C	40-6 3R	40-6 3C	40-6 4R	40-6 4C	40-6 5mc	40-8 1R
wt.%																		
SiO_2	51.4	52.0	52.2	52.6	52.6	52.8	51.4	51.3	52.2	52.0	52.3	52.1	51.7	54.4	53.4	51.1	50.3	52.4
TiO_2	0.48	0.44	0.56	0.43	0.34	0.40	0.48	0.50	0.47	0.58	0.41	0.56	0.48	0.30	0.32	0.57	0.72	0.32
Al_2O_3	2.42	2.09	2.24	2.38	2.70	2.23	3.21	3.07	2.71	2.97	3.32	2.94	3.32	1.42	1.71	3.82	4.06	2.58
FeO	7.36	6.82	7.25	6.27	5.48	5.92	6.85	7.31	6.09	5.98	4.63	4.85	5.12	6.08	5.37	5.04	5.21	8.13
Cr_2O_3	0.48	0.41	0.27	0.36	0.21	0.21	0.27	0.16	0.21	0.06	0.09	0.43	0.31	0.11	0.29	0.87	0.57	0.17
MnO	0.22	0.19	0.21	0.20	0.16	0.18	0.20	0.24	0.21	0.19	0.14	0.14	0.13	0.19	0.20	0.15	0.12	0.25
MgO	16.4	16.7	16.5	16.8	16.5	17.1	15.6	16.8	16.6	16.8	16.3	16.8	16.6	18.8	18.4	16.1	16.1	16.4
CaO	20.1	20.3	20.5	21.0	22.2	20.7	21.4	18.8	20.4	20.9	22.2	21.7	21.9	19.6	19.8	21.4	20.9	20.4
Na_2O	0.29	0.26	0.28	0.28	0.23	0.27	0.40	0.29	0.37		0.37	0.30	0.36	0.24	0.24	0.42	0.40	0.26
Total	99.2	99.2	100.0	100.3	100.4	99.8	99.7	98.5	99.8	99.9	100.4	99.8	100.0	101.0	99.7	99.6	98.3	100.9
mol.%																		
Ca	41.3	41.5	41.7	42.6	44.9	42.2	44.1	39.4	41.8	42.7	45.7	44.4	44.7	38.8	40.0	44.9	44.1	41.2
Mg	46.9	47.6	46.8	47.5	46.5	48.4	44.8	48.8	47.4	47.7	46.8	47.9	47.2	51.8	51.6	46.8	47.3	46.0
Fe	11.8	10.9	11.5	9.9	8.6	9.4	11.0	11.8	10.7	9.6	7.5	7.7	8.1	9.4	8.5	8.2	8.6	12.8

Sample	40-8 1C	40-8 2R	40-8 2C	40-8 3R	40-8 3C	40-8 4R	40-8 4C	40-10 1R	40-10 1C	40-10 2R	40-10 2C	40-10 3R	40-10 3C	40-10 4mc	40-10 5R	40-10 5C	40-10 6R*	40-10 7mc
wt.%																		
SiO_2	51.7	52.0	52.2	52.5	53.0	52.2	52.7	51.1	50.4	52.3	51.0	52.6	50.7	49.1	51.2	52.6	51.5	50.9
TiO_2	0.34	0.39	0.40	0.31	0.23	0.30	0.29	0.75	0.77	0.57	0.82	0.49	0.86	1.26	0.74	0.56	0.77	0.75
Al_2O_3	3.26	3.83	2.82	2.92	2.01	3.01	2.55	2.72	3.19	2.16	3.42	2.21	4.48	5.24	3.49	2.14	2.43	3.49
FeO	6.14	7.00	7.42	6.16	5.05	5.48	5.54	7.47	5.47	7.75	6.00	5.30	5.46	7.45	5.74	5.38	8.29	5.78
Cr_2O_3	0.42	0.26	0.23	0.25	0.43	0.39	0.41	0.05	0.72	0.09	0.57	0.47	0.55	0.24	0.50	0.44	0.08	0.52
MnO	0.19	0.20	0.23	0.22	0.15	0.15	0.16	0.24	0.17	0.24	0.18	0.19	0.16	0.19	0.19	0.18	0.28	0.19
MgO	16.1	15.7	15.8	16.2	16.3	16.3	15.7	16.1	15.6	17.2	15.9	17.1	15.5	15.1	15.9	16.9	17.4	15.0
CaO	21.5	21.7	21.4	22.2	22.6	22.3	21.5	19.8	21.2	18.9	21.6	21.4	21.2	20.1	21.2	21.3	18.1	21.4
Na_2O	0.24	0.23	0.24	0.20	0.19	0.18	0.25	0.31	0.35		0.36	0.30	0.46	0.42	0.40	0.31	0.25	0.39
Total	99.8	100.3	100.7	100.9	100.4	100.3	100.2	98.6	98.0	99.4	99.8	100.0	100.4	99.0	99.5	99.8	99.0	99.5
mol.%																		
Ca	44.2	44.2	43.6	44.9	45.4	45.3	43.9	41.2	44.9	38.8	44.6	43.4	44.4	42.9	44.3	43.5	37.1	44.4
Mg	45.9	44.6	44.6	45.4	45.8	46.0	47.3	46.7	46.1	48.8	45.7	48.2	45.1	44.7	46.3	47.9	49.6	46.2
Fe	9.9	11.2	11.8	9.7	7.9	8.7	8.8	12.1	9.1	12.4	9.7	8.4	10.6	12.4	9.4	8.6	13.3	9.4

mc= core of small crystal
R= rim of larger crystal
C= core of larger crystal
R*= rim around orthopyroxene

Table 5: Orthopyroxene Analyses

Sample	40-5 1R	40-5 1C	40-5 2R	40-5 2C	40-5 3mc	40-6 1R	40-6 1C	40-6 2mc	40-6 3mc	40-10 1R	40-10 1C	40-10 2R
wt.%												
SiO_2	53.7	53.7	54.1	53.9	53.9	53.9	54.1	51.9	55.6	55.1	56.4	53.5
TiO_2	0.10	0.13	0.11	0.16	0.16	0.12	0.11	0.15	0.10	0.12	0.14	0.15
Al_2O_3	0.52	0.56	0.53	0.41	0.52	0.46	0.45	0.62	0.41	1.04	0.47	0.47
FeO	18.9	18.7	18.6	18.9	18.3	18.9	18.6	18.6	18.1	12.8	11.6	19.1
Cr_2O_3	0.03	0.04	0.03	0.03	0.03	0.03	0.04	0.03	0.03	0.06	0.05	0.04
MnO	0.73	0.67	0.66	0.69	0.66	0.68	0.70	0.68	0.58	0.25	0.34	0.58
MgO	25.1	25.3	25.5	25.7	25.6	25.1	25.3	24.4	26.3	29.5	30.7	24.6
CaO	0.69	0.84	0.69	0.79	0.66	0.76	0.64	1.90	0.60	0.90	0.58	
Na_2O	0.02	0.02	0.02	0.03	0.03	0.03	0.03	0.03	0.03	0.04	0.04	0.04
Total	99.8	99.9	100.1	100.5	99.5	100.0	99.9	98.2	101.8	99.8	100.2	99.5
mol.%												
Ca	1.4	1.7	1.2	1.5	1.3	1.5	1.3	3.8	1.2	1.7	1.0	1.9
Mg	69.4	69.5	70.1	69.7	70.3	69.3	69.9	67.4	71.3	79.0	81.7	68.3
Fe	29.3	28.8	28.7	28.7	28.3	29.2	28.8	28.8	27.5	19.3	17.3	29.8

Sample	40-10 2C	40-10 3R	40-10 3C	40-10 4R	40-10 4C	40-10 5mc	40-16 1R	40-16 1C	40-16 2R	40-16 2C	40-16 3R	40-16 3C
wt.%												
SiO_2	54.2	53.7	54.1	53.8	54.6	53.1	53.7	54.1	54.1	53.9	54.8	55.0
TiO_2	0.11	0.10	0.11	0.12	0.10	0.13	0.15	0.14	0.13	0.12	0.10	0.14
Al_2O_3	0.42	0.40	0.39	0.61	0.35	0.57	1.03	0.64	0.59	0.77	0.56	0.57
FeO	18.9	18.9	18.7	19.2	18.6	19.1	17.7	17.9	18.3	18.2	17.6	17.2
Cr_2O_3	0.04	0.02	0.03	0.03	0.02	0.03	0.25	0.03	0.04	0.04	0.08	0.07
MnO	0.70	0.67	0.65	0.76	0.67	0.72	0.58	0.68	0.70	0.64	0.56	0.48
MgO	25.1	25.1	25.3	25.2	25.6	25.1	26.1	25.7	25.9	25.9	26.5	26.4
CaO	0.55	0.53	0.64	0.56	0.56	0.51	0.80	0.61	0.62	0.69	0.65	0.69
Na_2O	0.02	0.02	0.04	0.01	0.01	0.03	0.06	0.04	0.02	0.04	0.05	0.06
Total	100.1	99.4	99.9	100.2	100.5	99.2	100.2	99.8	100.4	100.8	100.8	100.7
mol.%												
Ca	1.1	1.0	1.3	1.1	1.1	1.0	1.6	1.2	1.2	1.4	1.3	1.4
Mg	69.5	69.7	69.8	69.2	70.2	69.4	71.8	71.0	70.8	70.8	72.0	72.2
Fe	29.4	29.3	28.9	29.7	28.7	29.6	27.1	27.8	28.0	27.9	26.8	26.4

mc= core of small crystal
R= rim of larger crystal
C= core of larger crystal

Table 6: Amphibole Analyses

Sample	40-5 1R	40-5 1C	40-5 2R	40-5 2C	40-5 3R	40-5 3C	40-5 4R	40-5 4C	40-5 5R	40-5 5C	40-6 1R	40-6 1C	40-6 2R	40-6 2C	40-6 3R	40-6 3C	40-6 4R	40-6 4C	40-6 5R	40-6 5C
wt.%																				
Na_2O	1.64	1.72	2.41	2.10	2.15	1.91	1.55	1.71	1.93	1.98	1.82	1.57	1.77	1.83	2.40	2.36	1.77	1.84	1.59	1.98
MgO	16.8	17.0	14.6	15.3	15.3	15.5	16.7	16.6	15.7	15.1	16.0	17.0	17.1	16.0	15.5	16.0	16.5	16.3	17.7	16.4
Al_2O_3	6.89	6.75	11.6	10.3	10.5	8.90	6.80	7.40	8.50	9.05	7.80	6.78	6.81	8.63	13.3	13.2	7.94	8.22	6.41	10.3
SiO_2	49.1	48.7	43.3	45.0	45.1	45.9	49.0	48.2	46.8	45.8	47.7	49.1	48.6	46.9	42.3	42.7	47.4	47.2	49.7	46.1
K_2O	0.32	0.32	0.44	0.44	0.34	0.47	0.35	0.34	0.39	0.55	0.39	0.34	0.33	0.34	0.85	1.02	0.36	0.36	0.24	0.42
CaO	11.4	11.3	11.7	11.7	11.7	11.6	11.1	11.4	11.5	11.5	11.9	11.9	11.6	11.8	12.3	12.2	11.9	11.9	11.4	12.2
TiO_2	1.51	1.38	2.52	1.36	1.29	1.92	1.45	1.52	1.65	2.12	1.83	1.57	1.42	1.75	1.93	1.90	1.62	1.89	1.24	1.33
Cr_2O_3	0.02	0.00	0.00	0.05	0.05	0.02	0.00	0.00	0.01	0.00	0.00	0.02	0.03	0.01	0.00	0.01	0.00	0.00	0.00	0.05
MnO	0.19	0.23	0.17	0.17	0.17	0.18	0.19	0.18	0.21	0.20	0.18	0.21	0.19	0.17	0.10	0.09	0.18	0.20	0.19	0.11
FeO	10.9	10.8	12.1	12.0	11.5	12.1	10.7	10.9	11.7	12.4	11.4	11.0	10.6	11.2	9.95	9.23	11.2	11.3	10.1	9.52
Cl	0.05	0.06	0.04	0.07	0.04	0.07	0.07	0.05	0.05	0.08	0.07	0.06	0.05	0.06	0.01	0.02	0.08	0.06	0.06	0.04
Total	98.8	98.3	99.0	98.5	98.2	98.6	97.9	98.3	98.4	98.8	99.0	99.5	98.4	98.7	98.7	98.7	99.0	99.3	98.6	98.4

Sample	40-10 1R	40-10 1C	40-10 2mc	40-10 3R	40-10 3C	40-10 4mc	40-10 5R	40-10 5C	40-10 6mc	40-16 1R	40-16 1C	40-16 2R	40-16 2C	40-16 3R	40-16 3C	40-16 4mc	40-16 5mc	40-16 6R	40-16 6C	40-16 7mc
wt.%																				
Na_2O	1.68	1.72	2.59	2.45	2.59	2.59	1.78	2.05	2.60	1.71	1.82	1.75	1.89	1.90	1.85	1.63	1.98	1.67	2.07	1.98
MgO	16.6	16.6	13.5	14.5	14.6	14.8	15.9	15.7	13.8	16.5	16.1	16.1	15.7	15.8	16.2	16.7	15.9	16.7	15.1	15.6
Al_2O_3	7.52	7.60	13.1	12.4	12.5	13.4	8.25	10.4	12.8	7.42	7.84	7.59	8.65	8.42	8.27	7.05	7.98	6.98	9.36	8.79
SiO_2	48.0	48.3	40.7	42.6	42.6	41.9	46.9	45.8	41.7	47.8	47.2	47.3	46.2	46.4	46.5	48.4	46.6	48.1	45.2	45.8
K_2O	0.32	0.32	0.46	0.50	0.45	0.48	0.34	0.28	0.41	0.32	0.34	0.39	0.39	0.35	0.41	0.31	0.38	0.33	0.44	0.43
CaO	11.7	11.8	11.8	11.8	11.6	11.9	11.7	11.9	11.3	11.6	11.6	11.7	11.7	11.6	11.9	11.6	11.7	11.5	11.7	11.7
TiO_2	1.59	1.63	4.00	3.50	3.36	3.86	1.72	1.38	3.49	1.59	1.72	1.89	1.80	1.76	1.92	1.42	2.20	1.37	2.21	2.07
Cr_2O_3	0.01	0.01	0.00	0.02	0.00	0.01	0.02	0.09	0.00	0.02	0.02	0.02	0.01	0.02	0.01	0.00	0.00	0.01	0.00	0.03
MnO	0.20	0.19	0.13	0.11	0.12	0.08	0.20	0.13	0.15	0.20	0.17	0.18	0.19	0.18	0.18	0.21	0.18	0.20	0.20	0.18
FeO	10.8	10.8	12.7	11.6	11.5	10.4	11.5	10.9	12.2	10.7	10.9	10.7	11.0	11.0	10.8	10.8	10.9	10.9	11.6	11.4
Cl	0.06	0.05	0.03	0.03	0.03	0.03	0.06	0.03	0.02	0.06	0.07	0.06	0.07	0.06	0.07	0.06	0.06	0.06	0.07	0.07
Total	98.4	99.1	98.9	99.3	99.3	99.4	98.3	98.7	98.6	97.8	97.7	97.6	97.7	97.5	98.1	98.2	97.8	97.4	97.9	98.0

mc= core of small crystal
R= rim of larger crystal
C= core of larger crystal

Table 7: Fe-Ti oxide Analyses

Sample	15-5	15-5	40-5	40-5	40-6	40-8	40-8	40-10	40-10	40-10	40-16
Occurrence	Gms	Gms	Gms	Opx	Gms	Gms	Gms	Plag	Opx	Opx	Gms
wt.%											
SiO_2	0.03	0.02	1.92	0.00	0.00	0.00	0.00	0.11	0.00	0.00	0.00
TiO_2	20.5	22.0	5.19	42.5	0.68	45.9	46.7	4.61	27.5	43.9	29.2
Al_2O_3	1.72	1.61	1.72	0.21	3.60	0.06	0.05	1.78	0.41	0.17	0.39
Cr_2O_3	0.02	0.02	0.53	0.00	0.49	0.00	0.00	0.02	0.00	0.02	0.07
Fe_2O_3	25.7	23.1	50.0	18.6	63.3	10.9	9.94	57.2	14.9	16.7	11.0
FeO	47.6	49.3	36.2	38.1	27.8	37.6	38.6	32.6	52.6	33.5	55.0
MnO	0.51	0.47	0.26	0.41	0.49	0.43	0.44	0.26	0.15	0.24	0.15
MgO	1.22	1.03	0.97	2.65	2.33	1.52	1.55	1.50	2.10	3.00	1.55
CaO	0.07	0.04	0.05	0.01	0.01	0.24	0.09	0.22	0.01	0.33	0.01
V_2O_3	1.15	0.85	0.68	0.48	0.65	0.51	0.40	0.52	0.45	0.38	0.46
Total	98.5	98.4	97.5	98.1	99.4	97.2	97.8	98.8	98.2	98.2	97.8
mol.%											
Usp	58.1	62.5	22.3	—	1.9	—	—	13.6	77.3	—	82.8
R_2O_3	—	—	—	18.2	—	10.7	9.7	—	—	16.2	—

Fe allocated to satisfy stoichiometry of $R^{2+}R^{3+}O_4$ for spinel (32 oxygens) or R_2O_3 for ilmenite (6 oxygens), using the method of Carmichael (1967). Gms= groundmass, Opx= orthopyroxene, Plag= plagioclase, Usp= ulvospinel.

Table 8: Conventional and $^{40}Ar/^{39}Ar$ K-Ar ages of dredged samples

(a) Conventional analyses

Sample No.	Material	K_2O (wt.%)	$^{40}Ar_{rad}$ ($x10^{-11}$ mol/gm)	$^{40}Ar_{rad}/^{40}Ar_{total}$	Calculated age (10^6 years)
40-5	Plag.	0.486 0.482	3.813	0.602	53.9±1.2
40-6	Plag.	0.409 0.409	3.115	0.546	52.1±1.2
40-7	Plag.	0.413 0.409	3.194	0.466	53.2±1.2
40-9	Plag.	0.407 0.403	2.970	0.492	50.2±1.5
40-10	Plag. (100-140)	0.410 0.403	3.120	0.430	52.5 → 53.3 ±1.1
40-10	Plag. (60-100)	0.405 0.406	3.208	0.447	54.1 → 53.3 ±1.1
40-16	Plag.	0.359 0.353	2.770	0.476	53.3±1.3
41-6	Plag.	0.281 0.290	2.281 2.264	0.407 0.591	54.6 → 54.4 ±1.2 54.2 →
45-4	WR	1.966 1.959	22.15 22.34	0.874 0.917	76.7 → 77.0 ±1.5 77.4 →
45-7	WR	0.898 0.900	6.443 6.397	0.334 0.119	49.0 → 49.0 ±1.2 48.8 →
15-5	Plag.	0.3225 0.3250	2.517	0.410	53.2±1.6
15-6	Plag.	0.3791 0.3762	2.920 2.921	0.404 0.197	52.9 → 52.9 ±1.0 52.9 →

(b) Total fusion experiment on amphibole 40-5

J	$^{40}Ar/^{39}Ar$	$^{37}Ar/^{39}Ar^*$	$^{36}Ar/^{39}Ar$	$^{36}Ar_{Ca}$ (%)	$^{39}Ar_{Ca}$ (%)	$^{40}Ar_K$ (%)	$^{40}Ar_R$ (%)	Calc. Age (10^6 years)
0.006311	19.518	11.417	0.05204	5.8	0.8	0.03	25.7	56.7±3.0

Table 8. Continued

(b) Analytical data for incremental heating experiment on plagioclase 40-16

Temp. (°C)	$^{40}Ar/^{39}Ar$	$^{37}Ar/^{39}Ar^{*}$	$^{36}Ar/^{39}Ar$	$^{36}Ar_{Ca}$ (%)	$^{40}Ar_{R}$ (%)	^{39}Ar (% of total)	Calc. Age (10^6 years)
J = 0.002319							
460	1251.5	3.607	4.192	0.0	1.0	1.3	53.7 ±76
550	87.02	6.052	0.2384	0.7	19.6	3.1	70.1 ±5.6
640	58.16	8.034	0.1328	1.6	33.6	4.9	80.4 ±3.4
710	20.02	9.535	0.02885	8.7	61.1	9.3	50.8 ±1.8
800	15.85	9.932	0.01314	20.0	80.4	18.7	52.9 ±0.9
900	15.05	9.971	0.01057	24.9	84.4	28.2	52.7 ±0.7
1010	14.93	9.766	0.01003	25.7	85.2	21.8	52.8 ±0.8
1350	25.57	9.305	0.04321	5.7	52.9	12.7	56.0 ±1.4
					Recalculated total fusion age= 54.9 ±1.1m.y.		

(d) Summary of age spectrum and isochron analyses

	Age spectrum		Isochron		
Increments used	Wt. mean age (10^6 years)	^{39}Ar (%)	Age (10^6 years)	Intercept	Sums/[N-2]
710 - 1350	53.0 ±0.5	90.7	52.1 ±1.0	312 ±15	1.49
710 - 1010	52.6 ±0.6	78.0	53.6 ±0.9	271 ±21	0.102
800 - 1350	53.0 ±0.5	81.4	51.9 ±0.7	320 ±11	0.022
800 - 1010	52.8 ±0.5	68.7	52.4 ±3.0	305 ±87	0.014

*Corrected for ^{37}Ar decay, half-life = 35.1 days. Subscripts indicate radiogenic (R), calcium-derived (Ca), and potassium-derived (K) argon. Lambda E = 0.581E-10/yr, lambda B = 4.692E-10/yr. Age constants: $\lambda_{e+e'} = 0.581 \times 10^{-10}$ yr^{-1}, $\lambda_{\beta} = 4.962 \times 10^{-10}$yr^{-1}, $^{40}K/K = 1.167 \times 10^{-1}$ atom percent.

Errors are estimates of the standard deviation of analytical precision.

Table 9a: Normalized Major element analyses of volcanic rock dredged from the continental margin in the Bering Sea on cruise L9-82-BS

Sample No.	40-5	40-8	40-9	40-10	40-16	41-6	45-4	45-7	47-8
Rock type	And.	Bas.	And.	And.	Dac.	And.	And.	Bas.	Bas.
Chem. class	med-K calc	med-K calc	med-K calc	med-K calc	med-K calc	med-K calc	high-K thol	med-K calc	med-K thol
(wt %)									
SiO_2	62.7	52.3	61.7	62.2	65.1	62.6	56.0	51.0	52.4
Al_2O_3	16.9	14.2	18.9	16.9	17.1	17.0	19.9	16.8	18.1
FeO*	4.40	8.50	3.71	4.32	3.25	5.44	4.66	8.14	8.33
MgO	3.39	8.06	2.45	3.36	2.76	2.23	1.69	3.44	5.15
CaO	5.31	12.2	5.40	5.83	4.62	5.10	8.72	8.32	9.44
Na_2O	4.45	2.25	5.16	4.18	4.67	4.32	4.04	4.28	3.39
K_2O	1.57	1.07	1.65	1.87	1.79	1.68	2.02	1.34	0.74
TiO_2	0.47	0.67	0.47	0.76	0.33	0.80	1.67	0.73	1.57
P_2O_5	0.43	0.20	0.23	0.35	0.15	0.29	0.71	0.56	0.32
MnO	0.05	0.14	0.03	0.07	0.04	0.05	0.06	0.06	0.12
Total	100.0	100.0	100.0	100.0	100.0	100.0	100.0	100.0	100.0
LOI	3.74	3.42	3.15	2.19	1.67	2.95	4.77	3.25	2.86
FeO*/MgO	1.30	1.05	1.52	1.28	1.18	2.45	2.75	1.50	1.62

FeO* is total iron as FeO
XRF analysis by A. Bartel and K. Stewart, proj. leader J. Taggart
LOI is loss on ignition at 900 ° C
And= andesite, B.and.= basaltic andesite, bas.= basalt, dac.= dacite, rhy.= rhyolite, chemical classification (thol= tholeiitic, calc= calc-alkaline) after Miyashiro (1974), and low-K, med-K, high-K after Gill (1981).

Table 9b: Major element analyses of volcanic rock dredged from the continental margin in the Bering Sea on cruise L5-78-BS

Sample No.	10-2	10-3	15-3	15-5	15-6	15-7	22-10	22-11
Rock type	Bas.	Bas.	B.And.	Bas	Bas.	Bas.	Rhy.	Rhy.
Chem. class	low-K thol	low-K thol	high-K thol	med-K calc	med-K calc	low-K thol	low-K calc	low-K calc
(wt %)								
SiO_2	49.3	49.4	53.4	51.2	52.4	52.3	71.4	71.0
Al_2O_3	15.9	15.8	18.3	17.3	18.5	17.3	13.1	13.8
Fe_2O_3	0.35	0.38	4.40	3.61	3.66	4.64	0.44	0.61
FeO	4.33	4.30	3.43	4.22	2.80	5.49	0.82	1.16
MgO	4.11	4.40	2.48	6.30	4.93	4.71	0.94	1.08
CaO	7.47	8.15	6.18	10.4	10.7	9.30	2.48	2.47
Na_2O	4.81	4.94	3.25	3.42	3.74	3.29	6.11	6.03
K_2O	0.05	0.03	2.45	1.03	1.34	1.08	1.32	1.37
TiO_2	1.72	1.71	1.09	0.95	1.02	0.84	0.20	0.20
P_2O_5	0.23	0.21	0.45	0.23	0.31	0.40	0.07	0.07
MnO	0.22	0.20	0.09	0.11	0.14	0.14	0.02	0.02
H_2O^+	4.13	2.70	0.82	0.75	0.64	0.91	0.42	1.25
H_2O^-	1.57	1.64	1.32	1.76	1.30	2.13	0.10	0.14
CO_2	0.09	0.06	0.05	0.07	0.05	0.08	0.07	0.04
Total	100.1	99.9	99.7	101.3	101.5	102.5	100.5	101.2
FeO^*/MgO	2.43	2.27	2.08	1.19	1.24	2.05	1.29	1.58

FeO^* is total iron as FeO
FeO, CO_2, H_2O by wet chemical analysis, B. Lai analyst, J.M. Baldwin proj. leader
other oxides by XRF analysis, S. Ramage analyst, V.G. Mossotti, proj. leader
abbreviations for rock types and chemical class as in Table 9a

Table 10a: Trace element analyses of volcanic rock dredged from the continental margin in the Bering Sea on cruise L9-82-BS

Sample No.	40-5	40-8	40-9	40-10	40-16	41-6	45-4	45-7	47-8
Rock Type	And.	Bas.	And.	And	Dac.	And.	B.And.	And	Bas.
Chem. class	med-K calc	med-K calc	med-K calc	med-K calc	med-K calc	med-K calc	med-K thol	high-K calc	med-K thol
*									
Ba	237	1360	246	1190	229	498	1245	302	242
Nb	7	5	<5	<5	<5	<5	11	6	5
Rb	33	22	14	31	20	32	40	24	13
Sr	566	353	611	597	570	838	843	569	437
Zr	134	51	139	160	135	117	180	132	119
Y	15	17	11	17	12	15	23	16	26
**									
Hf	3.1	1.2	3.3	3.5	2.9	2.6	4.3	3.6	2.7
Ta	0.16	0.07	0.18	0.24	0.12	0.17	0.51	0.23	0.25
Th	1.54	0.74	1.68	1.65	1.43	1.32	2.55	1.86	0.64
La	9.04	5.01	10.1	14.3	8.45	12.5	22.4	13.4	10.0
Ce	20.9	10.8	21.6	30.7	18.0	27.3	50.6	25.8	18.6
Nd	11.0	6.43	12.2	16.3	8.94	13.9	29.6	14.4	14.0
Sm	2.47	2.06	2.30	3.22	1.88	2.91	5.81	3.10	3.50
Eu	0.79	0.82	0.85	1.11	0.66	1.02	1.95	1.05	1.40
Tb	0.33	0.46	0.36	0.49	0.29	0.39	0.89	0.49	0.73
Yb	0.81	1.45	0.72	1.26	0.63	0.99	2.06	1.28	2.37
Lu	0.12	0.22	0.10	0.19	0.10	0.16	0.28	0.20	0.32
Sc	11	50	11	13	8.3	10	21	16	30
Co	17	43	11	16	10	10	16	29	32
Cr	67	446	54	89	34	18	18	90	226
Zr/Nb	19.1	10.2	27.8	32.0	27.0	23.4	16.4	22.0	19.8
K/Rb	395	404	978	501	512	436	419	463	473
K/Ba	55	6.5	56	13	65	28	14	37	25
$(Ba/La)_N$	2.5	27.1	2.5	8.4	2.7	4.0	5.6	2.3	2.4
$(La/Sm)_N$	2.1	1.0	2.4	2.4	2.5	2.4	2.1	2.3	1.6
La/Yb	11.9	3.5	14.0	11.4	13.4	12.7	10.9	10.5	4.2

*XRF analysis, R. Johnson and K. Dennen analysts, J. Lindsay proj. leader
** INAA analysis, J.S. Mee analyst, C.A. Palmer proj. leader
abbreviations for rock types and chemical classification as in Table 9

Table 10b: Trace element analyses of volcanic rock dredged from the continental margin in the Bering Sea on cruise L5-78-BS

Sample No.	10-2	10-3	15-3	15-5	15-6	15-7	22-10	22-11
Rock Type	Bas.	Bas.	B.And.	Bas.	Bas.	Bas.	Rhy.	Rhy.
Chem. class	low-K thol	low-K thol	high-K thol	med-K calc	med-K calc	med-K thol	low-K calc	low-K calc
*								
Ba	80	104	558	230	236	416	269	280
Nb	5	<5	<5	<5	27	32	<5	<5
Rb	2	2	50	22	29	20	18	20
Sr	132	120	524	325	354	396	827	832
Zr	78	76	107	83	80	67	76	79
Y	25	28	28	21	21	25	5	5
**								
Hf	2.3	2.3	3.1	2.0	2.1	2.2	2.2	2.3
Ta	<0.6	<0.6	0.31	0.37	0.38	0.26	0.15	0.16
Th	0.4	0.6	2.8	1.3	1.3	1.5	1.3	1.0
La	6	6	14	6.5	7.5	12.5	5	4
Ce	17	16	32	16	18	25	11	10
Nd	9	11	22	11	12	16	6	6
Sm	4.4	4.0	5.0	2.9	3.5	4.4	1.5	1.4
Eu	1.3	1.3	1.4	0.9	1.0	1.1	0.4	0.4
Tb	0.87	0.81	0.70	0.45	0.55	0.73	0.15	0.12
Yb	3.0	2.9	2.5	1.9	2.1	2.5	0.3	0.2
Lu	0.51	0.45	0.39	0.29	0.33	0.36	0.04	0.03
Sc	42	44	23	33	35	30	2.2	1.5
Co	37	35	20	30	37	28	3.4	3.3
Cr	139	132	21	223	228	35	17	16
Zr/Nb	15.6	<15	<21	<13	3	2	<16	<16
K/Rb	207	125	416	392	386	448	684	568
K/Ba	5.2	2.4	38	38	48	22	41	41
$(Ba/La)_N$	1.3	2.2	4.0	3.6	3.2	3.3	5.4	7.0
$(La/Sm)_N$	0.8	0.8	1.6	1.2	1.2	1.6	1.8	1.7
La/Yb	2.0	2.1	5.6	3.4	3.6	5.0	17	20

*XRF analysis, H.J. Rose, J. Lindsay, B. Mccall, R. Johnson analysts, H.J. Rose proj. leader
** INAA analysis, L.J. Schwarz analyst, P.A. Baedecker proj. leader
abbreviations for rock type and chemical classification as in Table 9

FIGURE CAPTIONS

Figure 1. Map of the Bering Sea continental shelf and slope showing dredge locations (circles).

Figure 2. Plagioclase compositions for dredged samples show a considerable range in An and Or content in a given sample. Or increases with decreasing An content, and An correlates in a general way with CaO content of the whole rock composition, shifting the range of compositions toward progressively lower An from basalt to andesite. However, andesite and dacite compositions overlap and show a larger compositional range with some crystal cores as calcic as those in basalt.

Figure 3. Pyroxene compositions for dredged samples on a Ca-Mg-Fe ternary diagram show a narrow range in clinopyroxene compositions with limited iron enrichment trend, especially for the basalt (field for andesites striped, for basalts stippled). Compositions of Aleutian clinopyroxene show a larger range but overlap compositions of the dredged samples. Orthopyroxene compositions of the dredged andesite and dacite are high Mg hypersthene with a narrow range in Wo.

Figure 4. Age spectrum and isochrons for $^{40}Ar/^{39}Ar$ incremental heating experiment for a plagioclase separate show concordant ages and a well defined plateau.

Figure 5. FeO^*/MgO ratio vs. SiO_2 in volcanic rocks dredged from the continental margin in the Bering Sea shows tholeiitic and calc-alkalic compositions (Miyashiro, 1974). Compositions of lava from the Aleutian arc are shown for comparison (shown as fields, data from Kay and others, 1982). Note that fields overlap in the range of basaltic compositions. Compositions of rocks from Bogoslof Island (squares), located some distance behind the Aleutian arc, have higher FeO^*/MgO ratios at a comparable SiO_2 content.

Figure 6. K_2O vs. SiO_2 in volcanic rocks dredged from the continental margin show most samples in the med-K compositional field of Gill (1981). Two samples are high-K, and the meta-basalt and rhyolite are low in potassium. Except for one high-K composition (15-3), all samples fall within the compositional range of Aleutian lava. Samples from Bogoslof Island are higher in potassium than Aleutian samples. Symbols and data for fields as in Figure 5.

Figure 7. Harker diagrams for the dredged samples show compositions similar to Aleutian volcanics. Na_2O (a) increases and Al_2O_3 (b), TiO_2 (c), and CaO (d) decrease with increasing SiO_2 but show considerable scatter, especially in the basaltic range. Symbols and data sources as in Figure 5.

Figure 8. Hf-Th-Ta plot for dredged samples shows all except the two meta-basalt samples in the field for convergent plate margin. The meta-basalt samples lie in the field for E-type MORB and oceanic island basalt (Fields after Wood and others, 1980).

Figure 9. Chondrite-normalized rare earth elements (REE) and Ba concentrations for dredged samples: (a) Basalt ($< 53\%$ SiO_2) show relatively flat profiles, whereas (b) more differentiated samples ($> 53\%$ SiO_2) show steeper slopes and light REE enrichment and lower heavy REE abundances. The meta-basalt (c) show flat profiles

with erratic spikes in the light REE region indicative of secondary alteration. The rhyolites (d) show very steep slopes and extremely low heavy REE abundances. Except for the meta-basalt, all samples show pronounced upward spikes for Ba characteristic for arc compositions. Values normalized to Leedy chondrite (Masuda and others, 1976).

Figure 10. Chondrite-normalized Ba/La vs. La/Sm plot for dredged samples shows high Ba/La ratios typical for arc compositions except for one of the meta-basalt which plots in the field for ocean floor basalt. Note sample 40-8 with a Ba/La ratio of 27 falls outside the figure. Fields for island arc and ocean floor basalt from Basaltic Volcanism Project (1981).

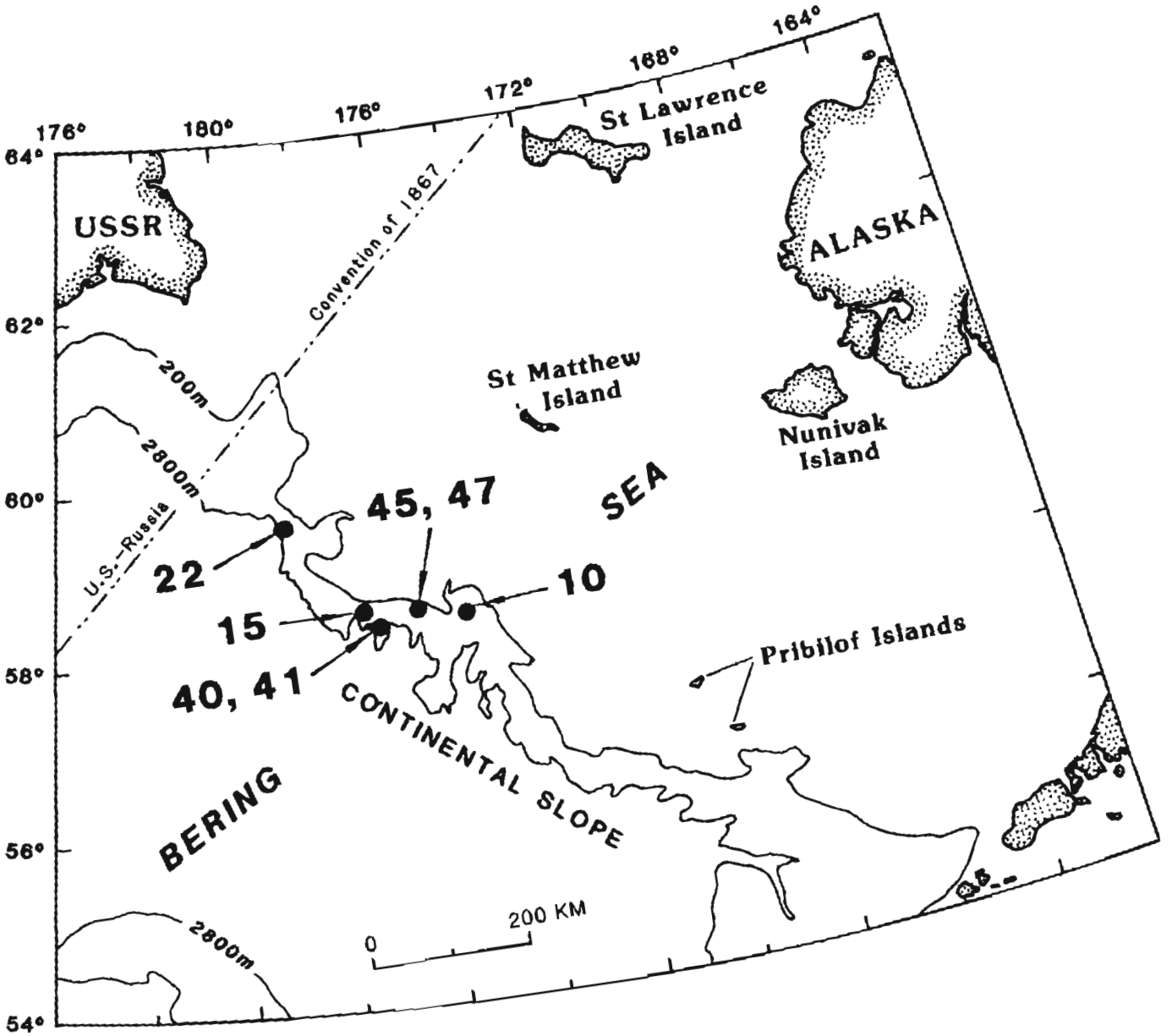
176°
180°
176°
172°
168°
164°
64°
62°
60°
58°
56°
54°
USSR
Convention of 1867
St Lawrence Island
ALASKA
St Matthew Island
Nunivak Island
200m
2800m
U.S.–Russia
45, 47
SEA
22
10
15
40, 41
CONTINENTAL SLOPE
Pribilof Islands
BERING
200 KM
0
2800m

Figure 1.

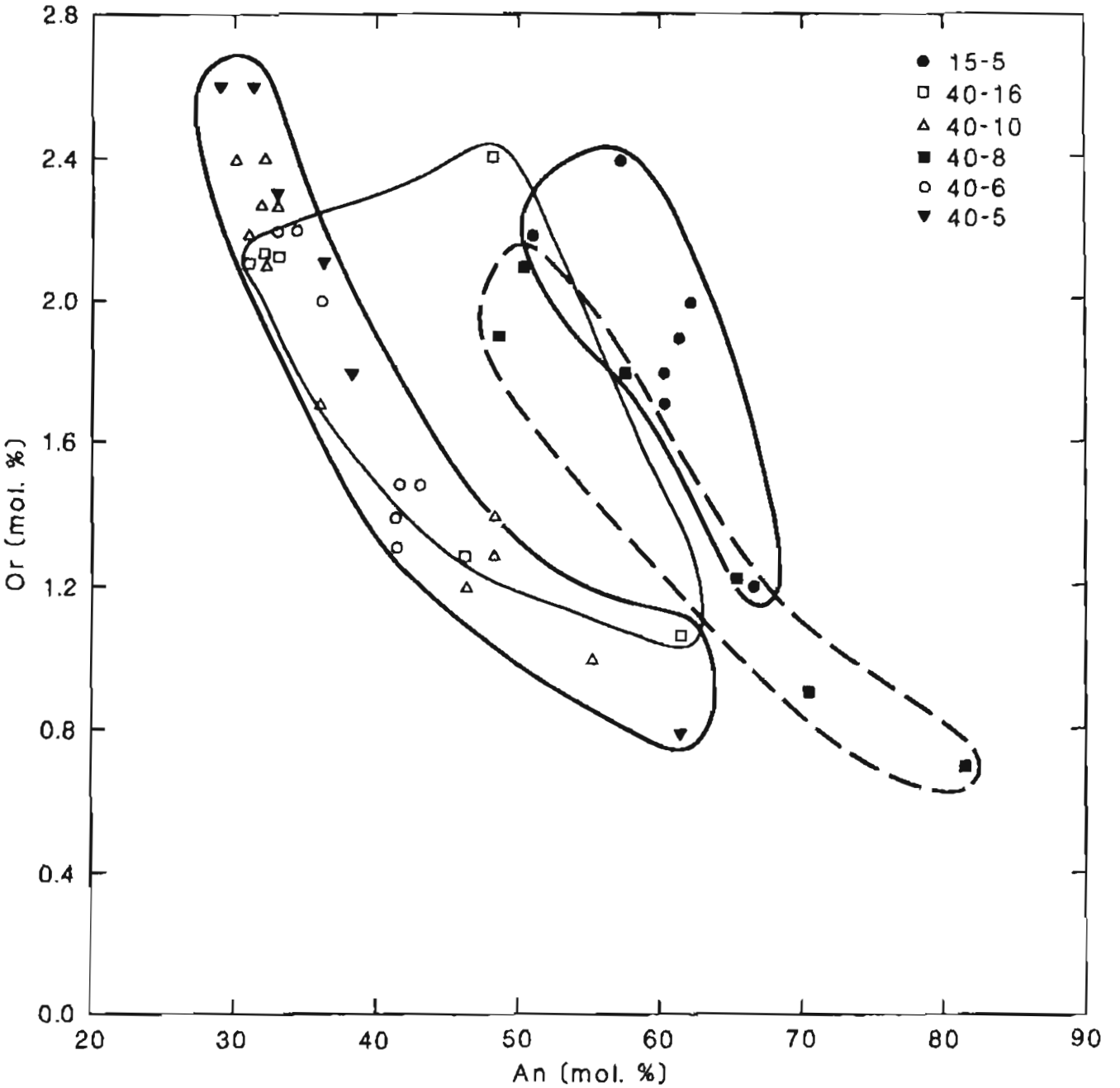
15-5
40-16
40-10
40-8
40-6
40-5
Or (mol. %)
An (mol. %)
0.0
0.4
0.8
1.2
1.6
2.0
2.4
2.8
20
30
40
50
60
70
80
90

Figure 2.

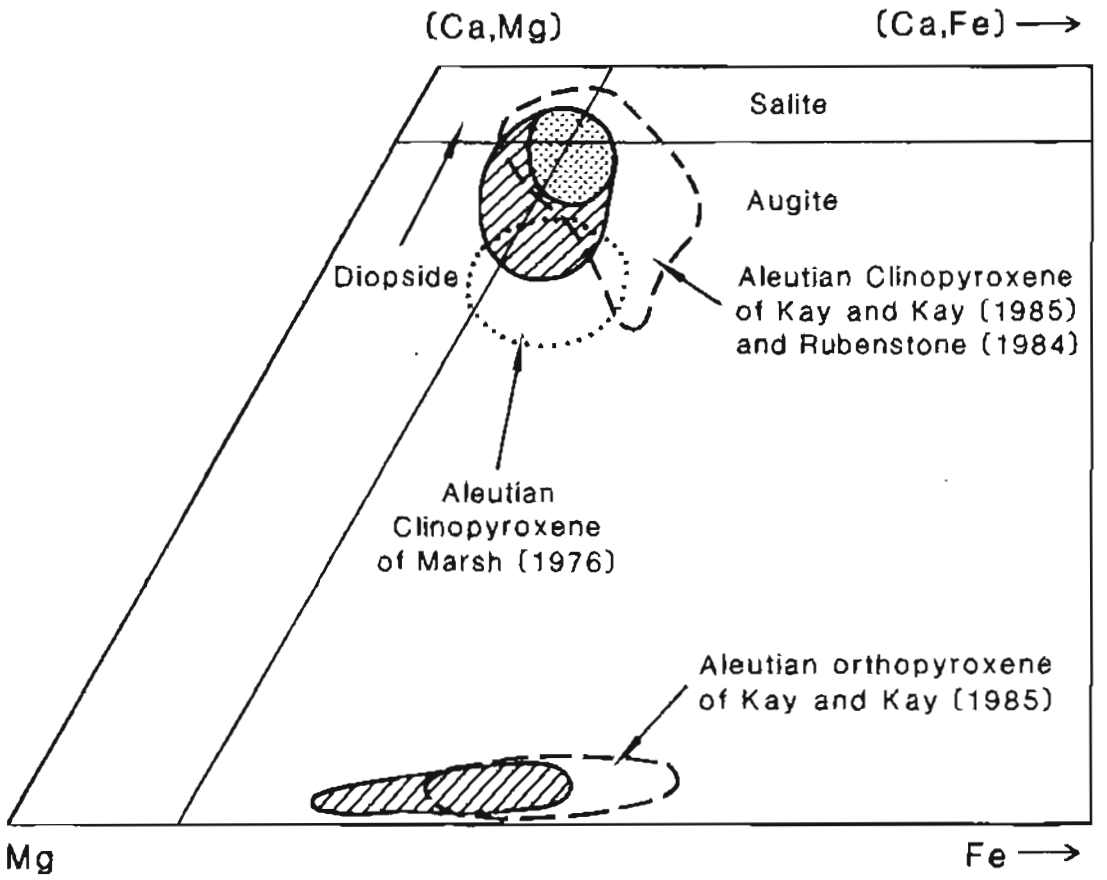
(Ca,Mg)
(Ca,Fe) ⟶
Salite
Augite
Diopside
Aleutian Clinopyroxene
of Kay and Kay (1985)
and Rubenstone (1984)
Aleutian
Clinopyroxene
of Marsh (1976)
Aleutian orthopyroxene
of Kay and Kay (1985)
Mg
Fe ⟶

Figure 3.

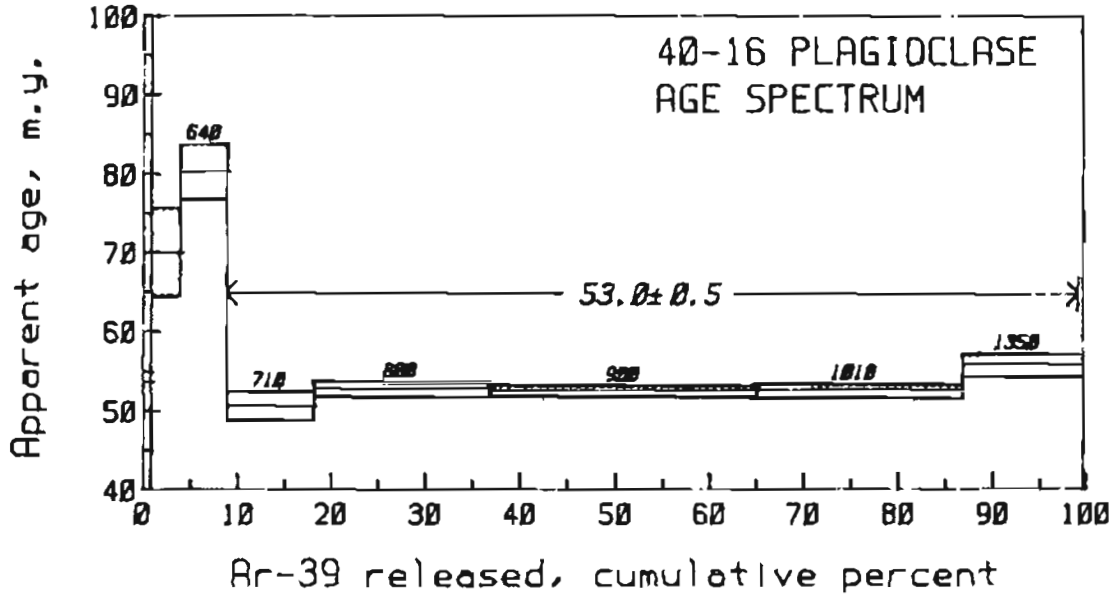
40-16 PLAGIOCLASE
AGE SPECTRUM
Apparent age, m.y.
100
90
80
70
60
50
40
640
53.0± 0.5
718
808
908
1018
1358
0
10
20
30
40
50
60
70
80
90
100
Ar-39 released, cumulative percent

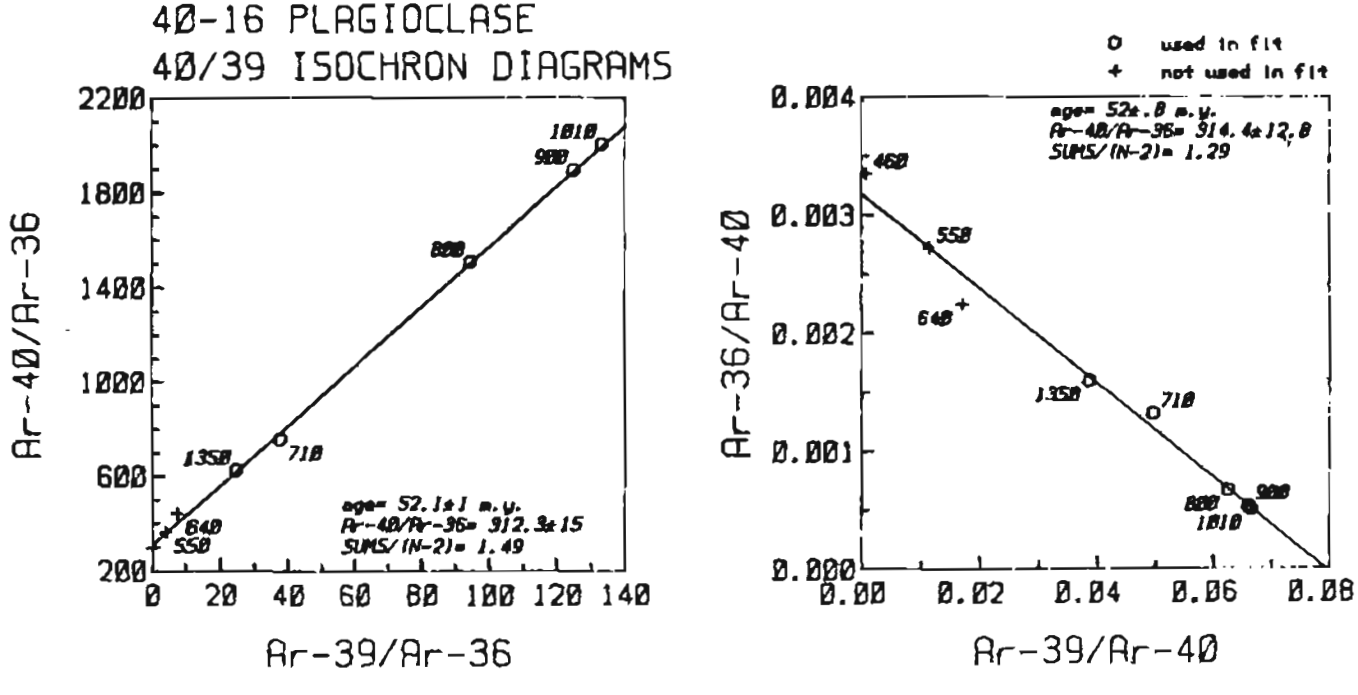
40-16 PLAGIOCLASE
40/39 ISOCHRON DIAGRAMS
Ar-40/Ar-36
2200
1800
1400
1000
600
200
1018
908
808
1358
718
640
550
age= 52.1± 1 m.y.
Ar-40/Ar-36= 312.3± 15
SUMS/(N-2)= 1.49
0
20
40
60
80
100
120
140
Ar-39/Ar-36
o used in fit
+ not used in fit
Ar-36/Ar-40
0.004
0.003
0.002
0.001
0.000
age= 52± .8 m.y.
Ar-40/Ar-36= 314.4± 12.8
SUMS/(N-2)= 1.29
460
558
640
1358
718
808
908
1018
0.00
0.02
0.04
0.06
0.08
Ar-39/Ar-40

Figure 4.

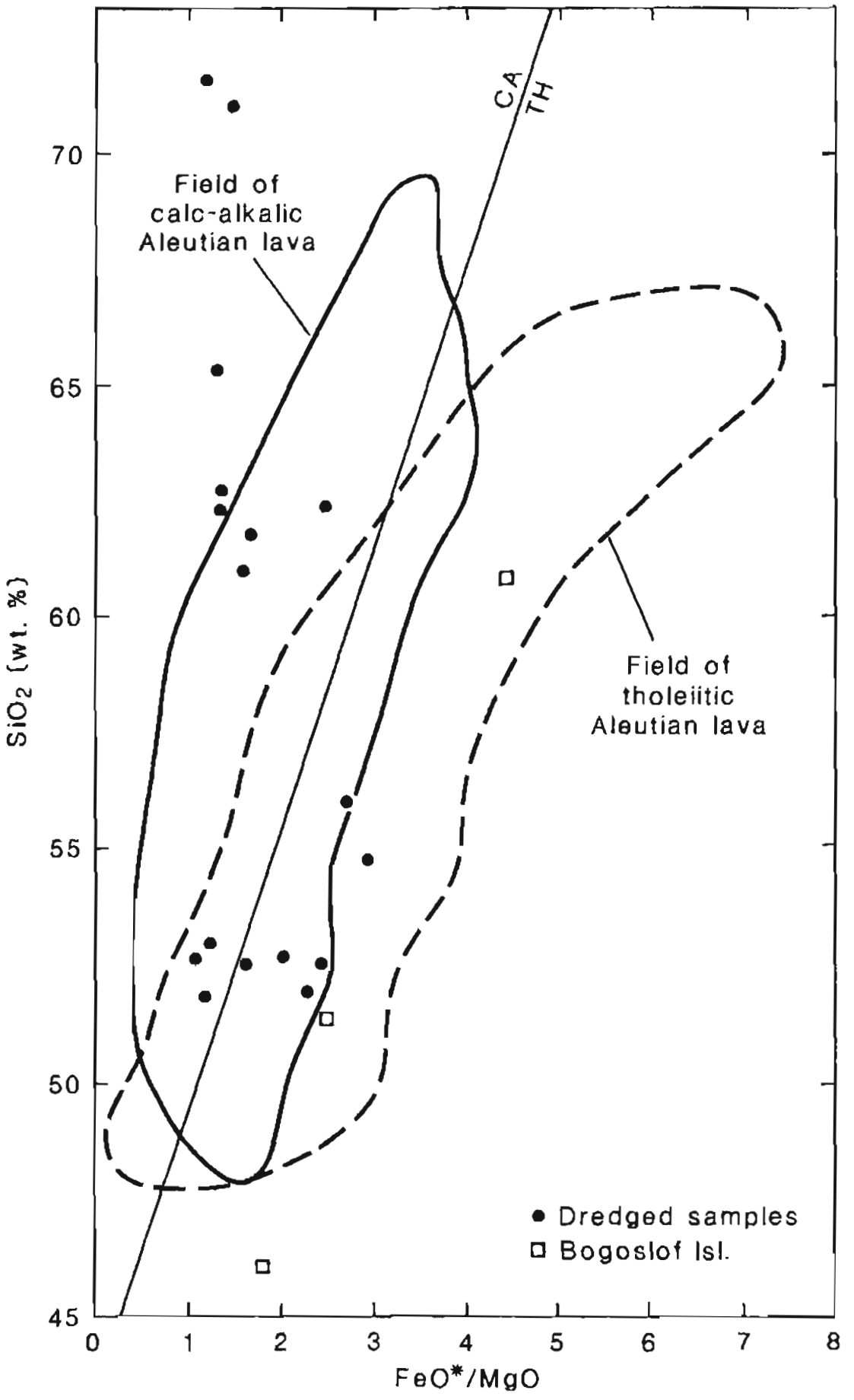
CA
TH
Field of
calc-alkalic
Aleutian lava
Field of
tholeiitic
Aleutian lava
Dredged samples
Bogoslof Isl.
SiO_2 (wt. %)
FeO*/MgO
70
65
60
55
50
45
0
1
2
3
4
5
6
7
8

Figure 5.

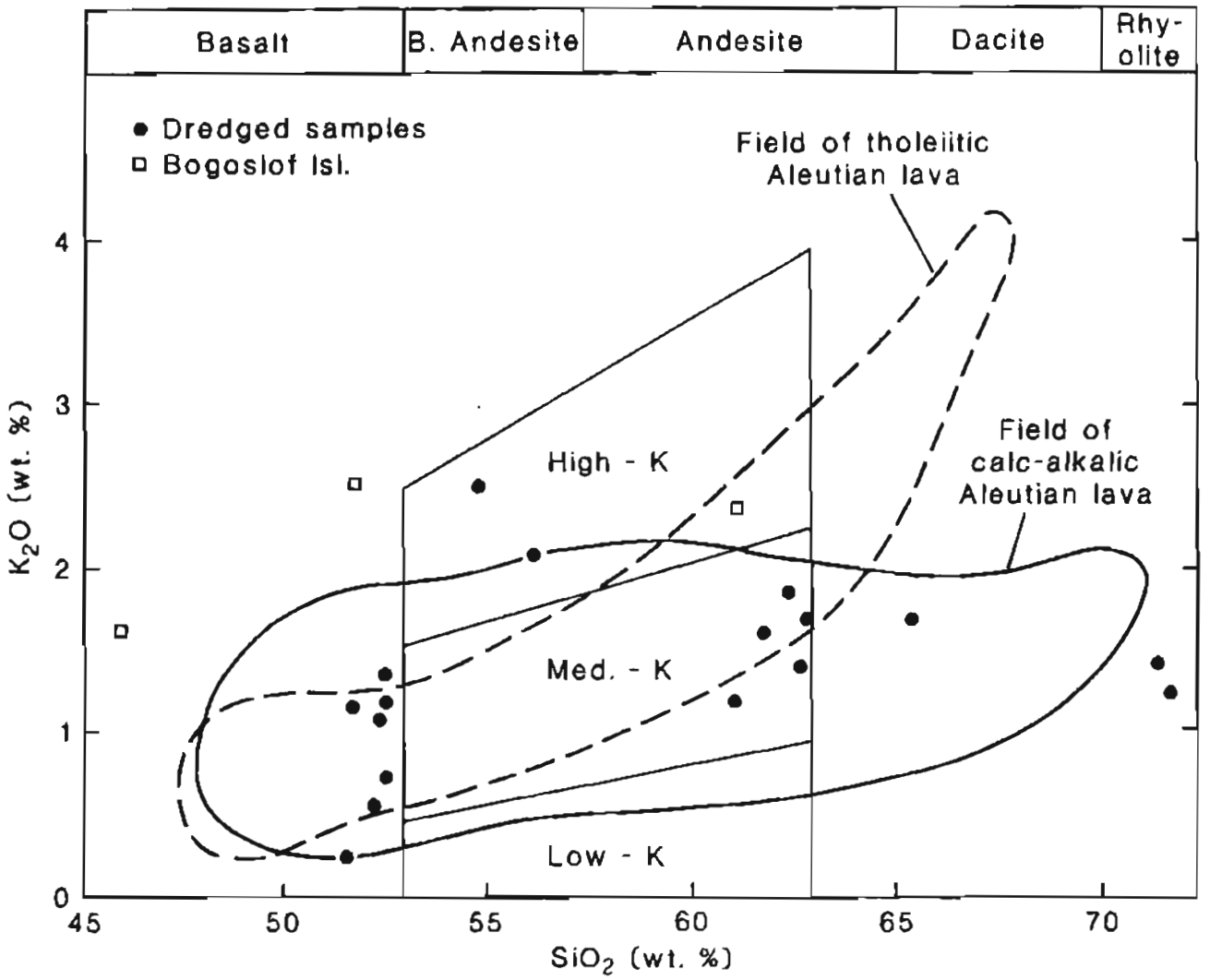
Basalt
B. Andesite
Andesite
Dacite
Rhy-olite
● Dredged samples
□ Bogoslof Isl.
Field of tholeiitic Aleutian lava
Field of calc-alkalic Aleutian lava
High - K
Med. - K
Low - K
K_2O (wt. %)
SiO_2 (wt. %)
0
1
2
3
4
45
50
55
60
65
70

Figure 6.

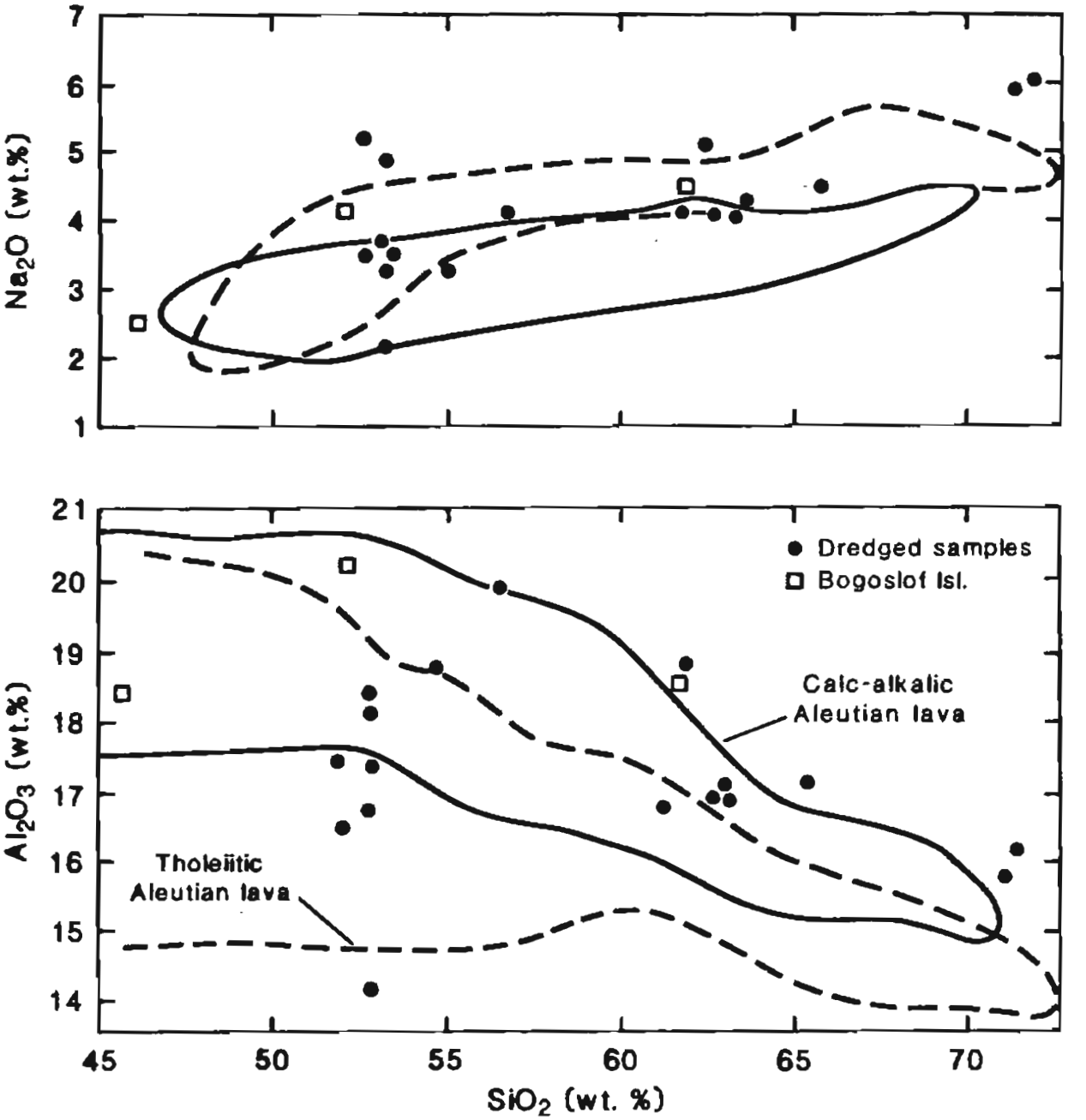
7
6
5
4
3
2
1
Na_2O (wt.%)
(a)
21
20
19
18
17
16
15
14
Al_2O_3 (wt.%)
Dredged samples
Bogoslof Isl.
Calc-alkalic
Aleutian lava
Tholeiitic
Aleutian lava
(b)
45
50
55
60
65
70
SiO_2 (wt. %)

Figure 7.

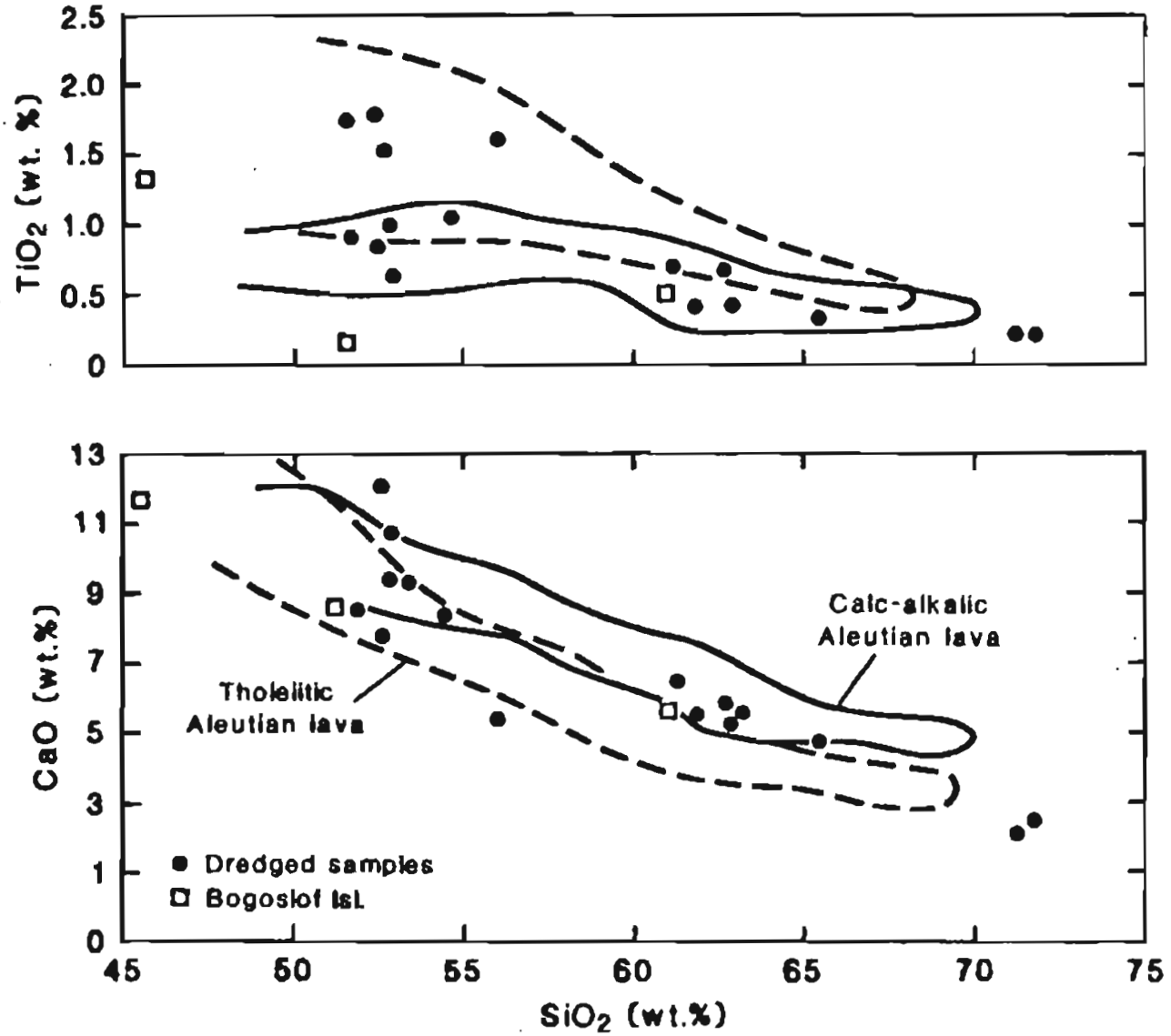
2.5
2.0
1.5
1.0
0.5
0
TiO2 (wt. %)
(c)
13
11
9
7
5
3
1
0
CaO (wt.%)
Calc-alkalic
Aleutian lava
Tholeiitic
Aleutian lava
Dredged samples
Bogoslof Isl.
(d)
45
50
55
60
65
70
75
SiO2 (wt.%)

Figure 7.

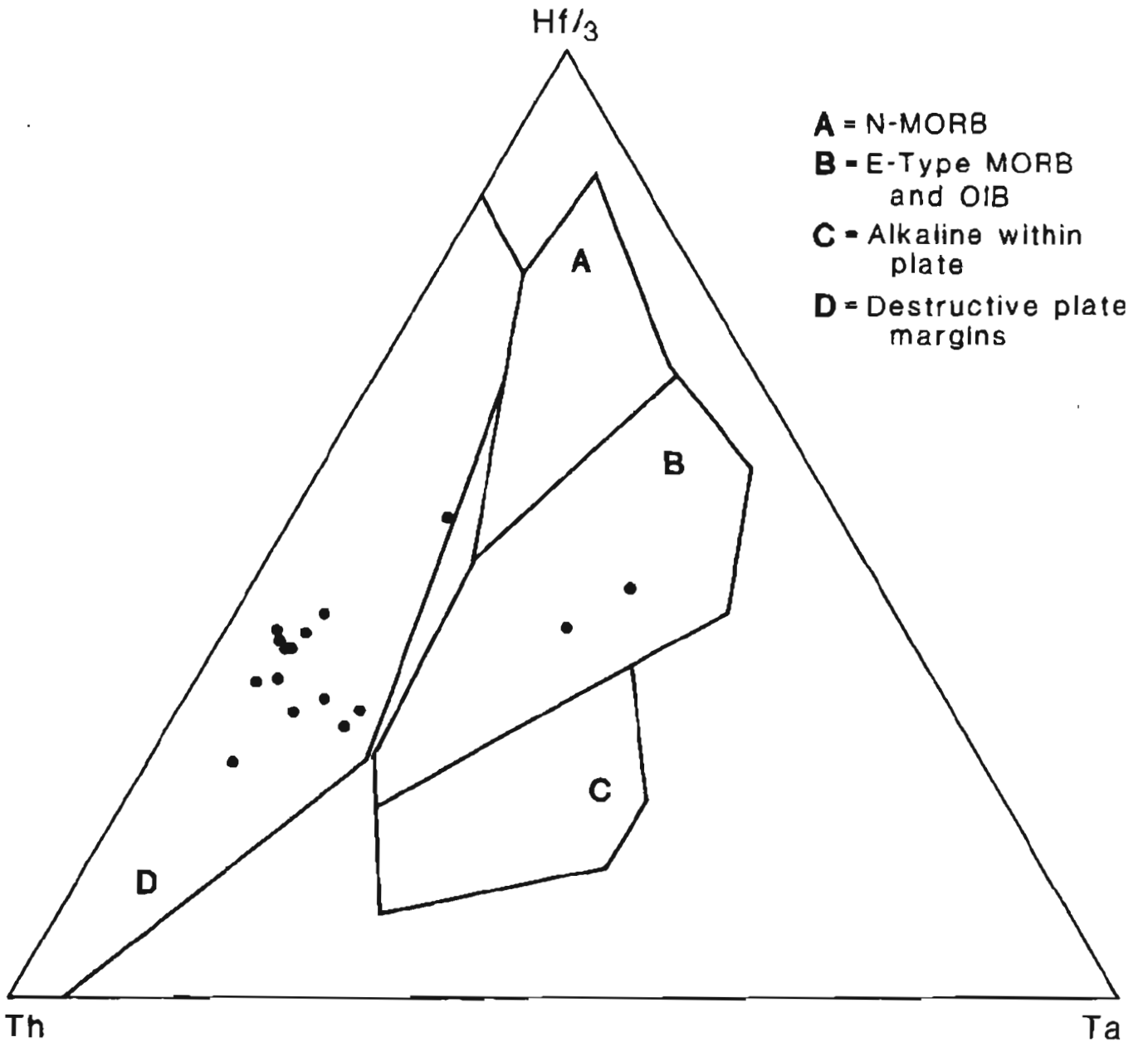
Hf/3
A = N-MORB
B = E-Type MORB and OIB
C = Alkaline within plate
D = Destructive plate margins
A
B
C
D
Th
Ta

Figure 8.

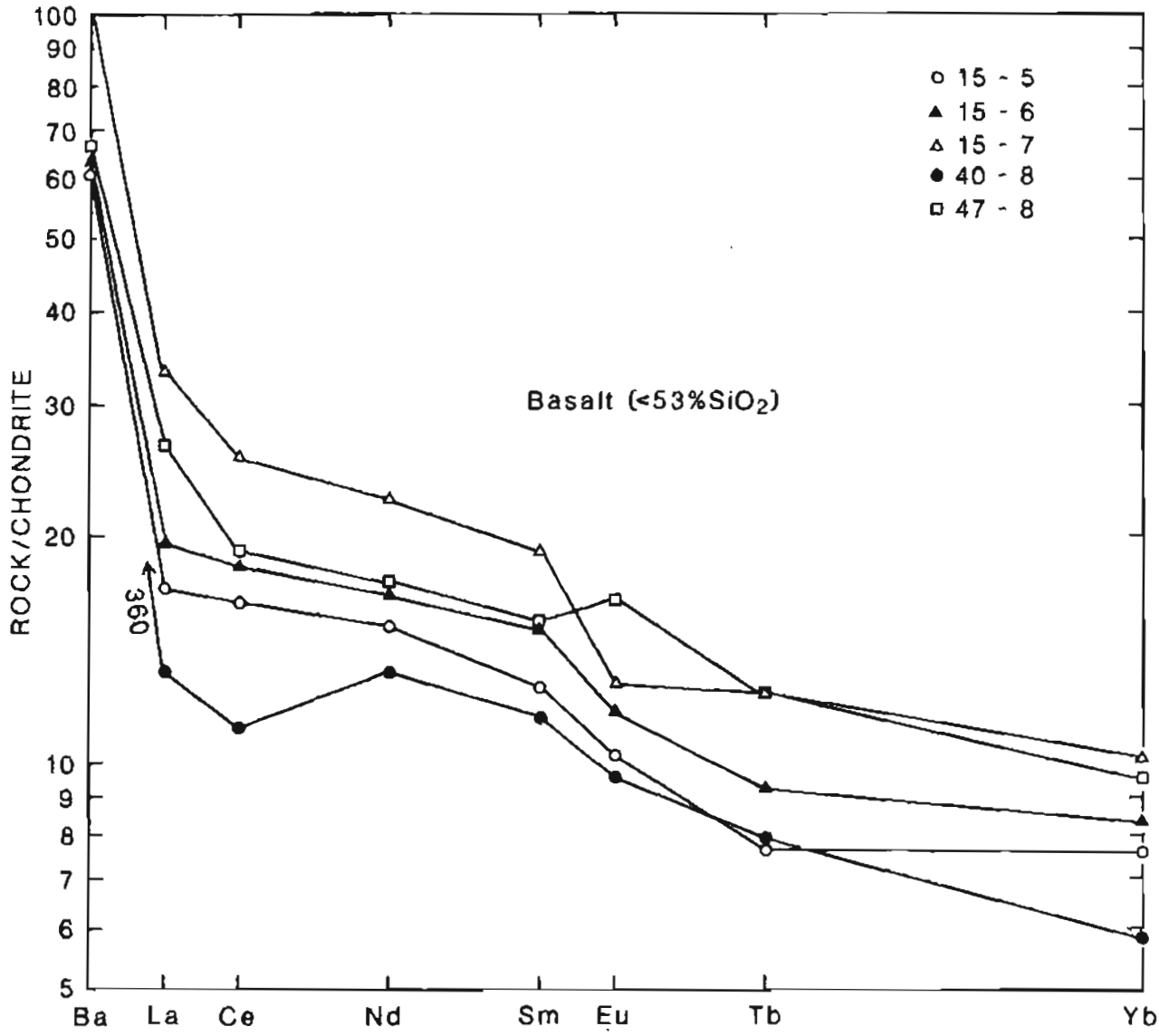
100
90
80
70
60
50
40
30
20
10
9
8
7
6
5
ROCK/CHONDRITE
Basalt (<53%SiO2)
15 - 5
15 - 6
15 - 7
40 - 8
47 - 8
390
Ba
La
Ce
Nd
Sm
Eu
Tb
Yb

Figure 9a.

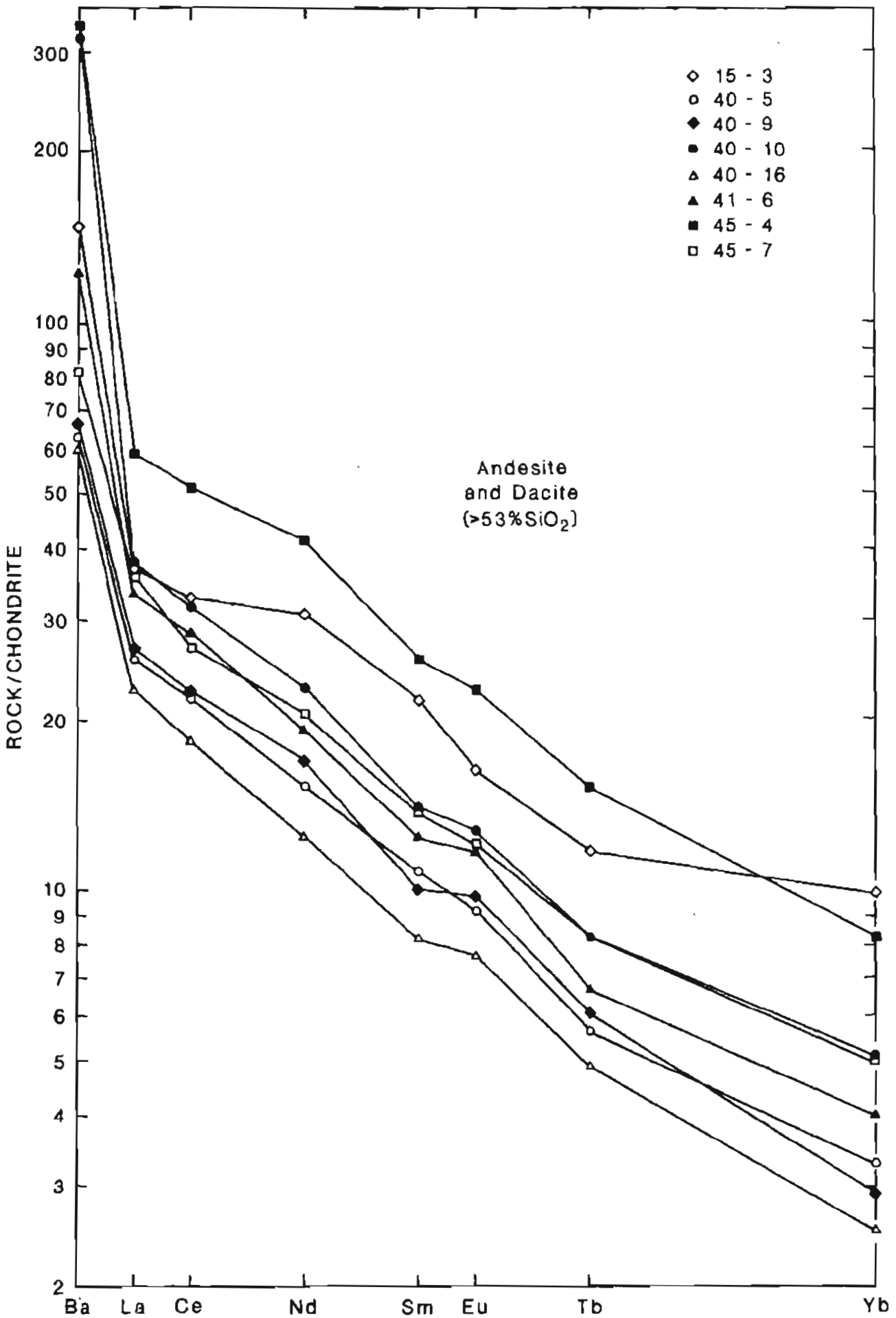
15 - 3
40 - 5
40 - 9
40 - 10
40 - 16
41 - 6
45 - 4
45 - 7
Andesite
and Dacite
(>53%SiO2)
ROCK/CHONDRITE
300
200
100
90
80
70
60
50
40
30
20
10
9
8
7
6
5
4
3
2
Ba
La
Ce
Nd
Sm
Eu
Tb
Yb

Figure 9b.

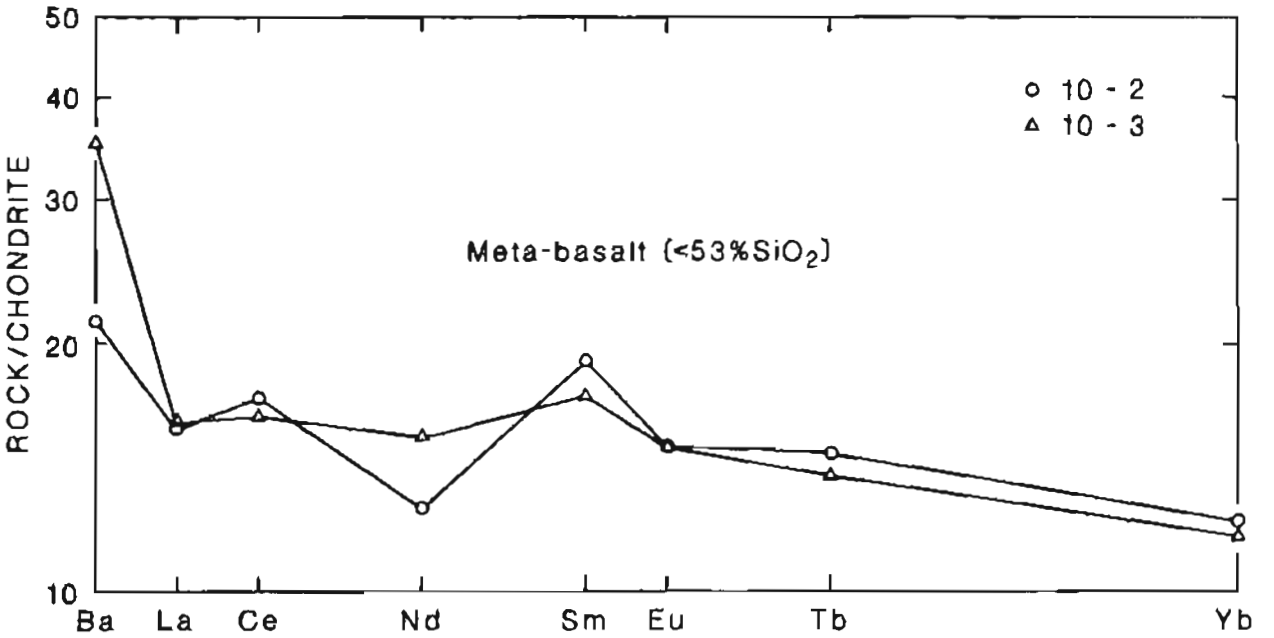
50
40
30
20
10
ROCK/CHONDRITE
Meta-basalt (<53%SiO2)
10 - 2
10 - 3
Ba
La
Ce
Nd
Sm
Eu
Tb
Yb

Figure 9c.

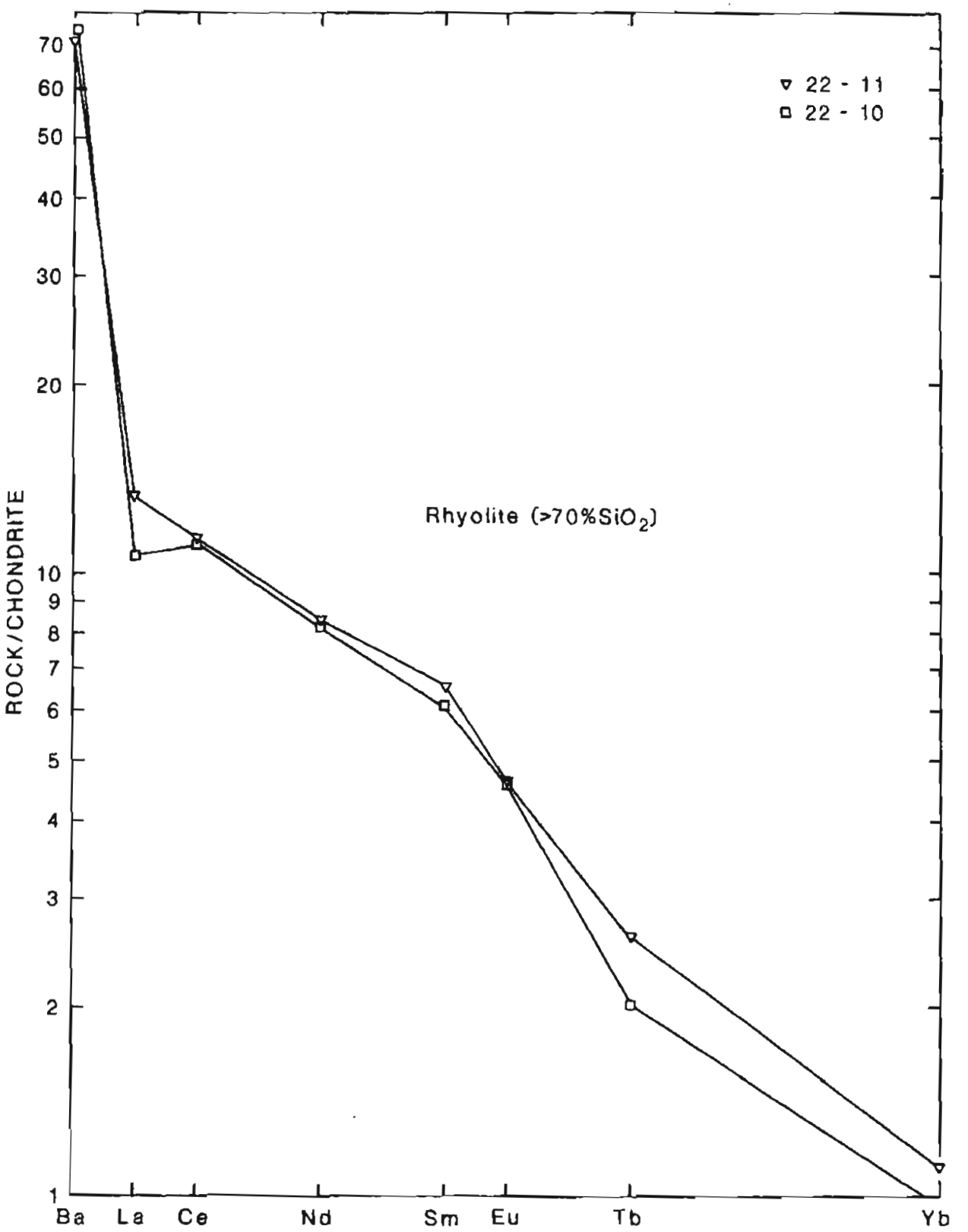
22 - 11
22 - 10
Rhyolite (>70%SiO2)
ROCK/CHONDRITE
70
60
50
40
30
20
10
9
8
7
6
5
4
3
2
1
Ba
La
Ce
Nd
Sm
Eu
Tb
Yb

Figure 9d.

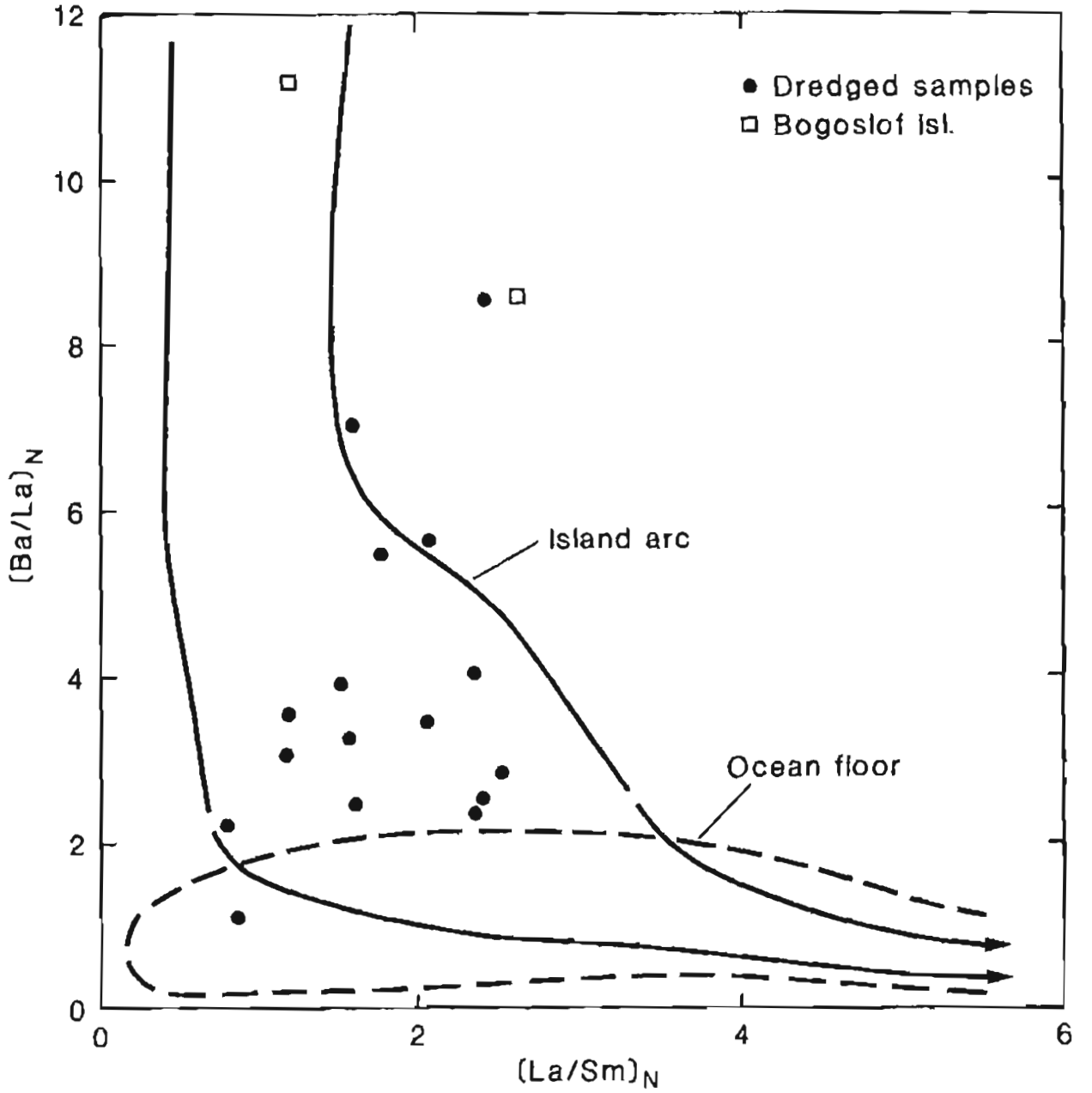
12
10
8
6
4
2
0
0
2
4
6
(Ba/La)N
(La/Sm)N
● Dredged samples
□ Bogoslof Isl.
Island arc
Ocean floor

Figure 10.